Electronic Supplementary Material (ESI) for Polymer Chemistry.

Electronic Supporting Information

Amine-bearing Cyclic Ketene Acetals for pH-Responsive and Degradable Polyesters through Radical Ring-Opening Polymerisation

Yiyi Deng[a,b], Anais Frezel[a,b], Fabian Mehner[a,b], Peter Friedel[a], Jens Gaitzsch[a,*]

[a] Leibniz-Institut für Polymerforschung Dresden e.V., Hohe Straße 6, 01069 Dresden, Germany

[b] TU Dresden, Bergstraße 66, 01069 Dresden, Germany

* Corresponding author: gaitzsch@ipfdd.de (J.G.)

Table of Contents

1 Materials and measurements 3

1.1 Materials 3

1.2 Measurements 4

2 Molecules synthesis and characterization 6

2.1 Synthesis of 2-(chloromethyl)-1,3,6-trioxocane 6

2.2 Synthesis of 2-methylene-1,3,6-trioxocane 7

2.3 Synthetic route towards amine-bearing CKAs (Alk-MACs) 8

2.4 Preparation of alkyl-substituted diethanolamine **3a-g** 9

2.5 Preparation of intermediate cyclic carbonate **5a-g** 11

2.6 Synthesis of Petasis reagent. 20

2.7 Synthesis of Alkyl-substituted-2-methylene-1,3,6-dioxazocane **7a-g** 21

2.8 2D HSQC NMR spectra of *sec*-butyl-derivatives and *iso*-propyl-derivatives 27

2.9 Optimization of alkyl-substituted diethanolamine preparation 28

2.10 Optimization of intermediate carbonate preparation 29

2.11 Theoretical calculation of Alk-MACs with the corresponding cyclic carbonate 30

3 Poly(Alk-MAC-co-MTC) preparation and characterization 32

3.1 Copolymerization of Alk-MACs and MTC 32

3.2 Conversion of ^{i}Pr-MAC **7c** and MTC 33

3.3 Final molar fraction of ^{i}Pr-MAC **7c** and MTC 35

3.4 ^{1}H NMR spectra of P(^{i}Pr-MAC-co-MTC) copolymers 36

3.5 ^{13}C NMR spectra of P(^{i}Pr-MAC-co-MTC) copolymers 37

3.6 DOSY measurement of P(^{i}Pr-MAC-co-MTC) 38

3.7 2D NMR measurements of P(^{i}Pr-MAC-co-MTC) 39

3.8 SEC measurements of poly(^{i}Pr-MAC-co-MTC) 41

3.9 Conversion of Alk-MAC and MTC 42

3.10 ^{1}H NMR of purified poly(Alk-MAC-co-MTC) 44

3.11 ^{13}C NMR of poly(Alk-MAC-co-MTC) 45

3.12 ATR-FTIR spectrum of Et-MAC-25T 46

3.13 SEC measurements of poly(Alk-MAC-co-MTC) 47

3.14 Molar mass and polymer dispersity of poly(Alk-MAC-co-MTC) 48

3.15 UV-vis transmittance measurements of copolymers 49

3.16 DLS measurement of ^{i}Pr-MAC-25T solution 55

3.17 Hydrolytic degradation of copolymers 56

4 References 60

1 Materials and measurements

1.1 Materials

Diethylene glycol (ReagentPlus grade, 99.0%), chloracetaldehyde dimethylacetal (≥ 99.0%, GC), DOWEX WX2 (hydrogen form, 100-200 mesh), *tert*-butanol (ACS reagent, ≥ 99.0%), potassium *tert*-butoxide (ACS reagent, ≥ 98.0%), diethanolamine (ACS reagent, ≥ 98.0%), *N*-ethyldiethanolamine (98.0%), *N*-butyldiethanolamine (≥ 98.6%), *N*-*tert*-butyldiethanolamine (97.0%), 2-bromopropane (99.0%), 1-bromopropane (99.0%), 2-methyl-1-bromopropane (98.0%), 2-bromobutane (98.0%), ethyl chloroformate (≥ 98%, GC), triethylamine (≥ 99.5%, GC), aluminum chloride (NH_4Cl, reagent grade, 98%), bis(cyclopentadienyl)titanium (IV)) dichloride (98.0%), methylmagnesium chloride solution (3M in THF) and potassium hydroxide (ACS reagent, 90%, ≥ 85%, pellets) were purchased from Sigma Aldrich and directly used without further purification. 2,2'-Azobis(2-methylpropionitrile) (AIBN, 98.0%) was purchased from Sigma Aldrich and re-crystallized in methanol for purification before usage. Sodium sulfate (Na_2SO_4, ACS reagent, ≥ 99.0%), magnesium sulfate ($MgSO_4$, ACS reagent, ≥ 99.0%) and sodium chloride (NaCl, ACS reagent, ≥ 99.5%) were purchased from Honeywell Fluka. Diethyl ether (99.5%) was purchased from CHEMSOLUTE. Methanol (99.5%), anhydrous tetrahydrofuran (THF, 99.5%), dichloromethane (> 99.8%) and chloroform (99.0%) were purchased from Acros Organics. Ethyl acetate (Analytical reagent grade, ≥ 99.8%) was purchased from Fischer Scientific. *N*-hexane (99.0%) was purchased from Supelco. Toluene (> 99.8%) was purchased from Thermo Scientific. Irgacure 184 was purchased from Ciba. Pre-treated RC dialysis membrane (MWCO: 1 k) was purchased from Carol Roth.

1.2 Measurements

Nuclear magnetic resonance spectroscopy (NMR). NMR spectra were acquired at a Bruker Avance III 500 MHz spectrometer with a frequency of 500 MHz for ^{1}H NMR and 125 MHz for ^{13}C NMR, and results were recorded at room temperature**.** HSQC was measured on a Bruker Avance III HD 600 MHz NMR-Spectrometer. $CDCl_3$ was used as solvent.

HSQC, HMBC and COSY measurements of copolymers ^{i}Pr-MAC-5T and ^{i}Pr-MAC-25T were performed on a Bruker Ultrafield DPX 400 MHz spectrometer. $CDCl_3$ was used as the solvent, ^{1}H peaks and ^{13}C peaks were reported using the shifts of residual $CHCl_3$ (7.26 ppm and 77.16 ppm respectively) as the internal standard. The DOSY experiments were performed at a Bruker Ultrafield DPX 500 MHz spectrometer

High resolution-mass spectrometry (HR-MS). HR-MS measurements were conducted on a 6200 series TOF/6500 series Q-TOF B.06.01 (B6172 SP1) under positive mode. ESI was used as ion source with methanol as solvent.

Attenuated Total Reflectance Infrared (ATR-FTIR) Spectroscopy. ATR spectra were acquired on a FT-IR spectrometer Vertex80v (Bruker) coupled with a single reflection Golden Gate Diamond ATR unit (SPECAC) and mercury cadmium telluride detector. The spectroscopic range was from 4000–600 cm^{-1} with 4 cm^{-1} spectral resolution, 100 scans.

Size-exclusion chromatography (SEC). SEC measurements were conducted at 25 ˚C with a PolarGel-M column (300 × 7.5 mm), using HPLC-Pump 1200 pump system (Aligent technologies) equipped with a multi angle laser light scattering (MALLS) detector (MiniDAWN TREOS II, Wyatt Technology) and a RI detector (K-2301 from KNAUER). DMAc with 3 g/L LiCl was used as an eluent and the flow rate was 1 mL/min. Before measurements, the samples were filtered with a 0.2 µm PTFE filter. The refractive index increments (d*n*/d*c*) were determined from RI signal through software Astra. All the copolymers were measured for two times.

UV transmittance measurements. pH responsiveness of copolymers was measured on a UV-VIS Specord Plus Spectrometer. Copolymers were dissolved into HCl solution in advance and then the solution was filtered with a PA 0.2 µm filter. The respective solution was adjusted to different pH values (0.1 M NaOH) and the % transmittance of the respective solution was recorded at 500 nm. For each sample, evolution of % transmittance with pH value was measured for three times and obtained data were combined to determine pH transition. Reduction of 50% transmittance of the solution was considered as transition pH.

Dynamic light scattering (DLS). The size distributions of copolymer against varying pH values were recorded by DLS measurements through a Zetasizer Nano-series instrument (Malvern Instruments, UK). The ^{i}Pr-MAC-25T/HCl solution was titrated by adding 0.1 M NaOH dropwise tuning the pH value from 2.4 to 9. DLS measurements were performed at 25 °C and data were collected by NIBS method (non-invasive back-scatter) with a helium–neon laser (4 mW, l = 632.8 nm) at fixed scattering angle of 173 °.

Hydrolysis degradation measurements. Hydrolysis degradation was studied under accelerated condition. In a vial, 25 mg copolymer was dissolved in 1.0 mL THF and 0.5 mL 5 wt% KOH/MeOH was added into vial subsequently. The mixture was stirred at room temperature for 24 h. Then the solvent was removed under reduced pressure and the degraded copolymer was characterized using NMR spectroscopy and SEC measurements.

Computational method. All the optimization calculations of molecules were conducted by the software package GAMESS with the basis set STO-6G.[1] The calculations were performed simulating conditions of 0 K and vacuum.

2 Molecules synthesis and characterization

2.1 Synthesis of 2-(chloromethyl)-1,3,6-trioxocane

Diethylene glycol (70 mL, 739 mmol, 1.0 eq.), chloracetaldehyde dimethylacetal (94 mL, 826 mmol, 1.1 eq.) and DOWEX WX2(1.01 g) were mixed in a two-necked flask and degassed with nitrogen for 5 min. The reaction mixture was stirred at 120 °C in a gentle nitrogen stream and the methanol formed during the reaction was collected in a collection flask. The reaction was stopped when no more methanol was formed (after about 2 h). The crude product was subsequently purified by recondensation (75-80 °C, 3 mbar). The white, crystalline product was obtained. (76.5 g, 459 mmol, 62%).

^{1}H NMR (500 MHz, $CDCl_3$) δ (ppm) 4.78-4.80 (t, *J* = 5.4 Hz, 1H, OCHO), 3.92-4.03 (m, 4H, OCH_2), 3.61-3.80 (m, 4H, OCH_2), 3.46-3.49 (d, *J* = 6.4 Hz, 2H, CH_2Cl).

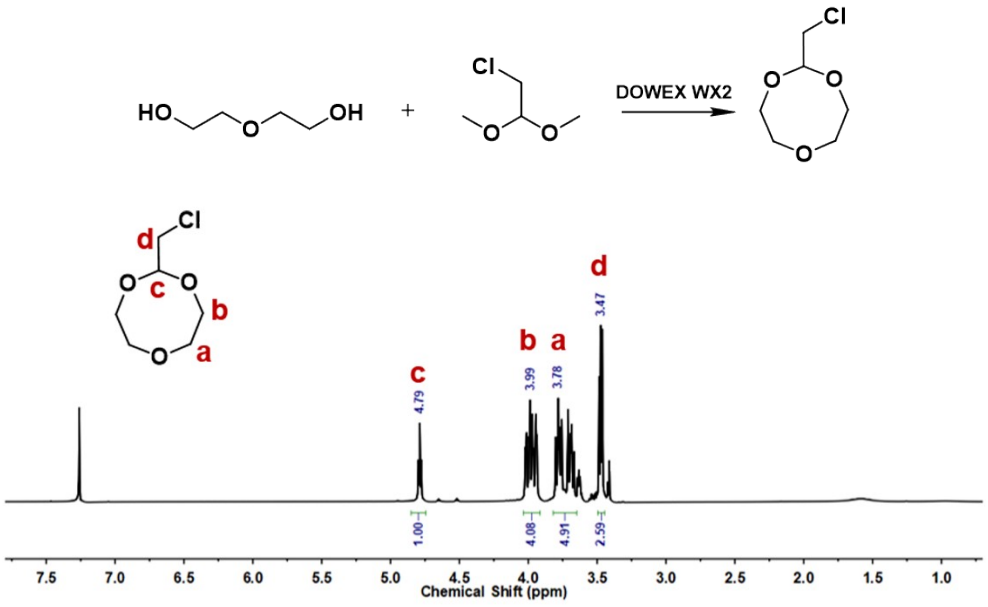

Figure S1. ^{1}H NMR spectrum of 2-(chloromethyl)-1,3,6-trioxocane**.**

2.2 Synthesis of 2-methylene-1,3,6-trioxocane

2-(Chloromethyl)-1,3,6-trioxocane (20.0 g, 120 mmol, 1.0 eq.) and *tert*-butanol (HO^{t}Bu, 61.6 mL) were charged in a Schlenk tube and degassed with nitrogen for 15 min. Potassium *tert*-butoxide (KO^{t}Bu, 16.16 g, 144 mmol, 1.2 eq.) was added slowly. The mixture was stirred at 120 °C for 16 h. The product was washed with diethyl ether and the precipitated KCl was filtered off with a Büchner funnel. Then the crude product was purified by 3 successive distillations (70 °C, 20 mbar). 2-Methylene-1,3,6-trioxocane (MTC) was obtained as a colorless liquid (53%).

^{1}H NMR (500 MHz, $CDCl_3$) δ (ppm) 4.05-4.07 (t, *J* = 4.8 Hz, 4H, OCH_2), 3.76-3.78 (t, *J* = 4.8 Hz, 4H, OCH_2), 3.67 (s, 2H, C-CH_2).

^{13}C NMR (125 MHz, $CDCl_3$) δ (ppm) 164.03 (1C, $\underline{C}CH_2$), 70.99 (1C, $C\underline{C}H_2$), 70.50 (2C, OCH_2), 70.40 (2C, OCH_2).

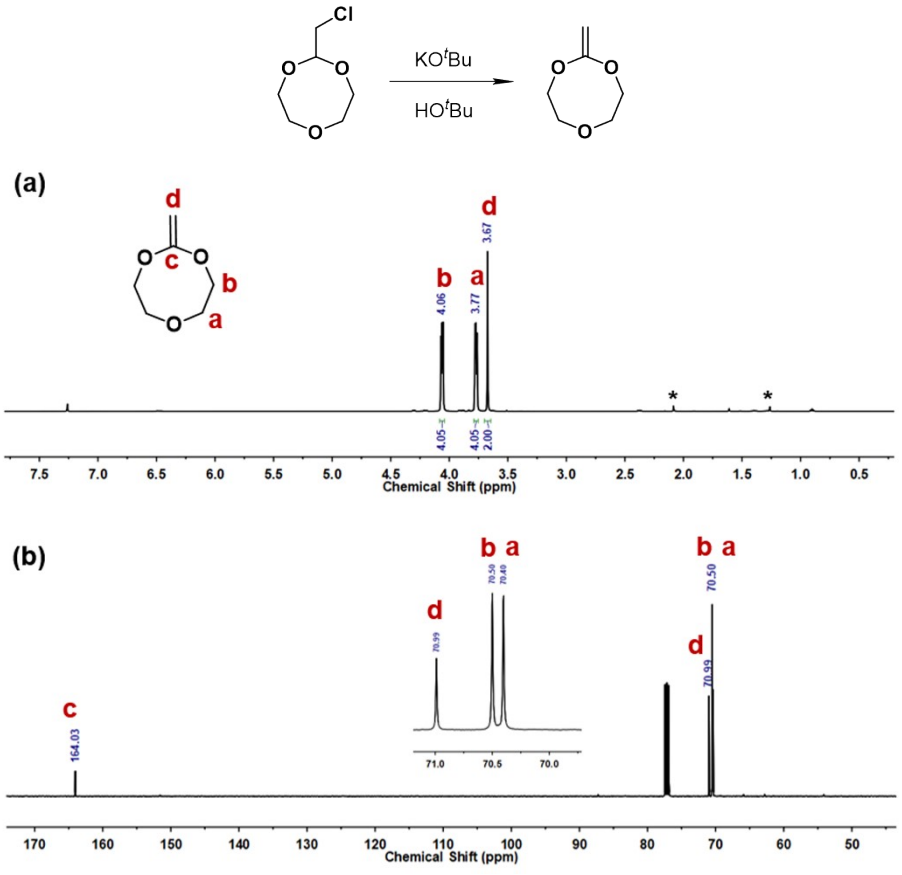

Figure S2. (a) ^{1}H NMR and (b) ^{13}C NMR spectra of 2-methylene-1,3,6-trioxocane.

2.3 Synthetic route towards amine-bearing CKAs (Alk-MACs)

Amine-bearing CKAs (Alk-MACs) were prepared following a similar synthetic procedure proposed by our group.[2] The synthetic route consists of alkylation step, cyclization step and methylenation step, which will be introduced in the following.

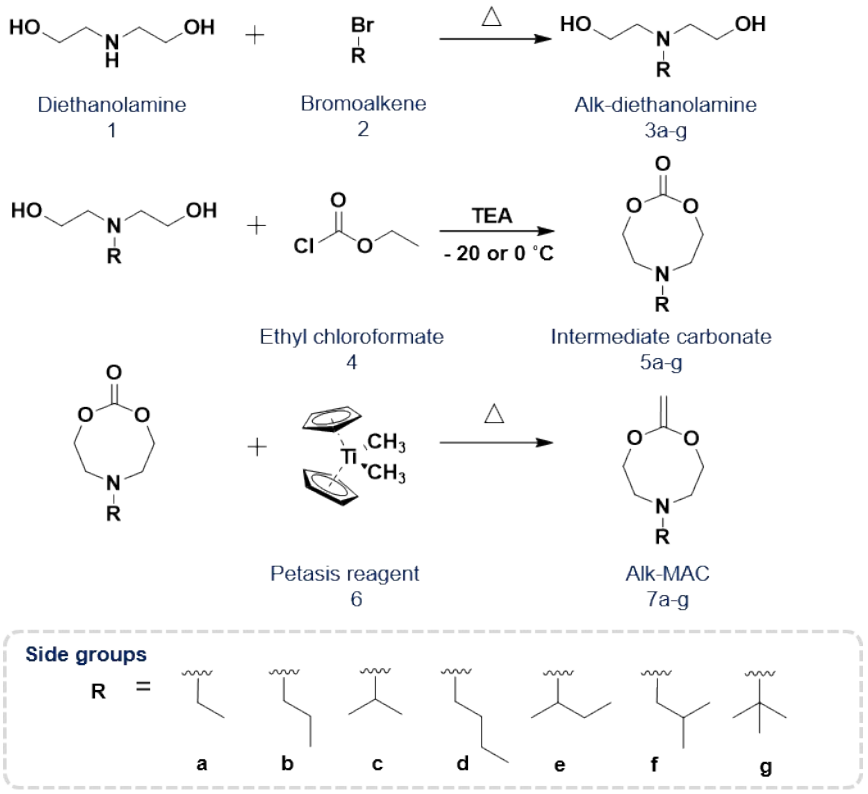

To make it brief, alkyl-substituted diethanol amines were labelled as **3a-g**. All the as-prepared intermediate carbonates are abbreviated to "alkyl-cyclic carbonate" in the following, also labelled as **5a-g**. For example, 6-butyl-1,3,6-dioxazocan-2-one is named as ^{n}Bu-cyclic carbonate. Similarly, all the newly synthesized Alk-MACs are named as "alkyl-substituted-MAC", labelled as **7a-g**. For example, 6-butyl-2-methylene-1,3,6-dioxazocane is named as ^{n}Bu-MAC.

2.4 Preparation of alkyl-substituted diethanolamine **3a-g**

Diethanolamine (8.8 g, 83.7 mmol, 1.0 eq.) and bromoalkene (1.0 eq.) were charged into a round bottom flask and the mixture was heated up to 65-90 ℃ under argon protection. After stirring for 72 h, the reaction mixture was cooled to room temperature and then KOH solution (4.8 g/10 mL H_2O) was added and kept stirring for 5 min. Subsequently, water was removed under reduced pressure. The mixture was diluted with 10 mL methanol and kept stirring for another 5 min. After isolating KBr through filtration paper, methanol was removed under reduced pressure and the concentrated crude product was washed with 2 mL toluene (two times). The toluene phases were disposed and then the mixture was extracted with dichloromethane (20 mL for 3 times). The organic phases were collected and concentrated afterwards. After dried in the vacuum oven overnight, a yellow oil was obtained.

***N*-Ethyldiethanolamine (3a)** was commercially available.

***N*-propyldiethanolamine (3b). ^{1}H NMR** (500 MHz, $CDCl_3$) δ (ppm) 3.60-3.62 (t, *J* = 5.6 Hz, 4H, OCH_2), 2.70 (s, 2H, OH), 2.64-2.66 (t, *J* = 5.4 Hz, 4H, NCH_2), 2.47-2.50 (t, *J* = 7.6 Hz, 2H, $NC\underline{H}_2CH_2CH_3$), 1.45-1.52 (m, 2H, $NCH_2C\underline{H}_2CH_3$), 0.87-0.90 (t, *J* = 7.2 Hz, 3H, $NCH_2CH_2C\underline{H}_3$). **^{13}C NMR** (125 MHz, $CDCl_3$) δ (ppm) 59.85 (2C, OCH_2), 56.91 (1C, $N\underline{C}H_2CH_2CH_3$), 56.27 (2C, NCH_2), 20.42 (1C, $NCH_2\underline{C}H_2CH_3$), 11.84 (1C, $NCH_2CH_2\underline{C}H_3$).

***N-iso*-propyldiethanolamine (3c). ^{1}H NMR** (500 MHz, $CDCl_3$) δ (ppm) 3.69-3.49 (t, *J* = 5.4 Hz, 4H, OCH_2), 3.09-2.89 (m, 1H, NCH), 2.80-2.67 (br, 2H, OH), 2.65-2.56 (t, *J* = 5.4 Hz, 4H, NCH_2), 1.09-0.94 (d, *J* = 6.6 Hz, 6H, N(CH)-CH_3). **^{13}C NMR** (125 MHz, $CDCl_3$) δ (ppm) 60.24 (2C, OCH_2), 51.67 (2C, NCH_2), 51.07 (1C, NCH), 18.24 (2C, N(CH)-CH_3).

***N*-Butyldiethanolamine (3d)** was commercially available.

***N-sec*-Butyldiethanolamine (3e). ^{1}H NMR** (500 MHz, $CDCl_3$) δ (ppm) 3.54-3.62 (t, *J* = 5.4 Hz, 4H, OCH_2), 2.66-2.71 (m, 1H, $N(CH_3)C\underline{H}CH_2CH_3$), 2.56-2.62 (m, 4H, NCH_2), 2.53 (br, 2H, OH), 1.47-1.56, 1.25-1.34 (m, 2H, $N(CH_3)CHC\underline{H}_2CH_3$), 0.98-0.99 (d, *J* = 6.6 Hz, 3H, $N(C\underline{H}_3)CHCH_2CH_3$), 0.91-0.94 (t, *J* = 7.2 Hz, 3H, $N(CH_3)CHCH_2C\underline{H}_3$). **^{13}C NMR** (125 MHz, $CDCl_3$) δ (ppm) 60.23 (2C, OCH_2), 57.66 (1C, $N(CH_3)\underline{C}HCH_2CH_3$), 51.63 (2C, NCH_2), 26.78 (1C, $N(CH_3)CH\underline{C}H_2CH_3$), 14.35 (1C, $N(\underline{C}H_3)CHCH_2CH_3$), 11.75 (1C, $N(CH_3)CHCH_2\underline{C}H_3$).

***N-iso*-Butyldiethanolamine (3f). ^{1}H NMR** (500 MHz, $CDCl_3$) δ (ppm) 3.59-3.62 (t, *J* = 5.4 Hz, 4H, OCH_2), 2.62-2.64 (m, 1H, NCH), 2.60 (br, 2H, OH), 2.25-2.26 (d, *J* = 7.2 Hz, 2H, $NCH_2CH(CH_3)_2$), 1.70-1.81 (m, *J* = 6.6 Hz, 1H, $NCH_2C\underline{H}(CH_3)_2$), 0.89-0.91 (d, *J* = 6.6 Hz, 6H, $NCH_2CH(C\underline{H}_3)_2$). **^{13}C NMR** (125 MHz, $CDCl_3$) δ

(ppm) 63.82 (1C, N<u>C</u>H_2CH(CH_3)$_2$), 59.72 (2C, OCH_2), 56.74 (2C, NCH_2), 26.56 (1C, NCH_2<u>C</u>H(CH_3)$_2$), 20.75 (2C, NCH_2CH(<u>C</u>H_3)$_2$).

***N-tert*-Butyldiethanolamine (3g)** was commercially available.

^{1}H and ^{13}C NMR spectra of alkyl-substituted diethanolamine

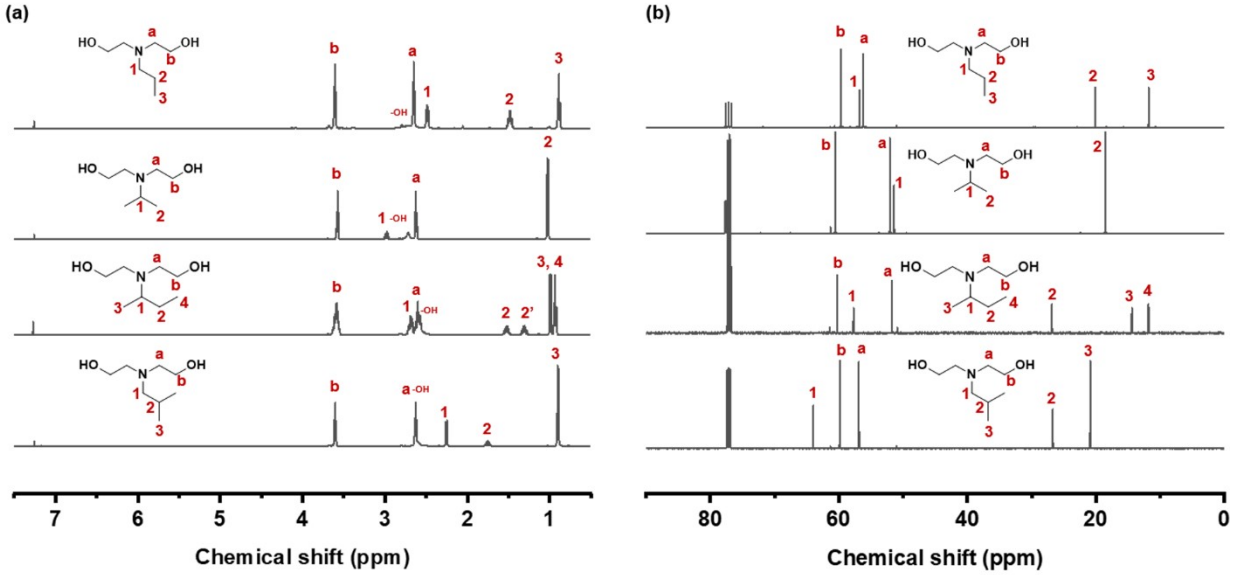

Figure S3. (a) ^{1}H and (b) ^{13}C NMR spectra of alkyl-substituted diethanolamine **3b, 3c, 3e** and **3f**. Substances **3a**, **3d** and **3g** are commercially available and therefore the NMR spectra were not shown here.

2.5 Preparation of intermediate cyclic carbonate **5a-g**

Alkyl-substituted-diethanolamine (1 eq.) was dissolved in anhydrous THF and then the mixture was flushed with argon, chilled in an ice bath and stirred for 30 min. Ethyl chloroformate (2.5-6.2 eq.) was added into the flask and kept stirring for another 30 min. Subsequently, TEA (2-4 eq.) dried over Na_2SO_4 was added into the flask using a syringe pump with a feeding speed of 20-400 μL/min. The mixture was stirred in an ice bath for 2 h and another 17 h at room temperature. The precipitations were filtered off and then the solvent was removed under reduced pressure. The crude product was purified using column chromatography (n-Hexane/EtOAc = 3/1) and the aimed substance was obtained as yellow oil.

6-Ethyl-1,3,6-dioxazocane (5a). **^{1}H NMR** (500 MHz, $CDCl_3$) δ (ppm) 4.17-4.19 (t, *J* = 5.0 Hz, 4H, OCH_2), 2.77-2.79 (t, *J* = 5.4 Hz, 4H, NCH_2), 2.69-2.74 (t, *J* = 7.2 Hz, 2H, NCH_2CH_3), 1.03-1.06 (d, *J* = 7.2 Hz, 3H, CH_3). **^{13}C NMR** (125 MHz, $CDCl_3$) δ (ppm) 156.27 (1C, CO), 69.15 (2C, OCH_2), 53.99 (2C, NCH_2), 50.87 (1C, NCH_2CH_3), 12.25 (1C, CH_3). **HR-MS (ESI)** m/z calculated for $C_7H_{13}NO_3$ ([M+H]+), **160.0968**, found, **160.0969**; calculated for $C_7H_{13}NO_3$ ([M+Na]+), **182.0788**, found, **182.0786.**

6-Propyl-1,3,6-dioxazocane (5b). **^{1}H NMR** (500 MHz, $CDCl_3$) δ (ppm) 4.17-4.19 (t, *J* = 5.4 Hz, 4H, OCH_2), 2.79-2.81 (t, *J* = 5.4 Hz, 4H, NCH_2), 2.57-2.60 (t, *J* = 7.2 Hz, 2H, $NC\underline{H}_2CH_2CH_3$), 1.43-1.51 (m, 2H, $NCH_2C\underline{H}_2CH_3$), 0.85-0.88 (t, *J* = 7.2 Hz, 3H, $NCH_2CH_2C\underline{H}_3$). **^{13}C NMR** (125 MHz, $CDCl_3$) δ (ppm) 156.20 (1C, CO), 69.20 (2C, OCH_2), 59.00 (1C, $N\underline{C}H_2CH_2CH_3$), 54.27 (2C, NCH_2), 20.80 (1C, $NCH_2\underline{C}H_2CH_3$), 11.46 (1C, $NCH_2CH_2\underline{C}H_3$). **HR-MS (ESI)** m/z calculated for $C_8H_{15}NO_3$ ([M+H]+), **174.1125**, found, **174.1119**; calculated for $C_8H_{15}NO_3$ ([M+Na]+), **196.0945**, found, **1196.0943.**

6-(*iso*-Propyl)-1,3,6-dioxazocane (5c). **^{1}H NMR** (500 MHz, $CDCl_3$) δ (ppm) 4.17 (t, *J* = 5.4 Hz, 4H, OCH_2), 2.95 (m, 1H, NCH), 2.74 (t, *J* = 5.0 Hz, 4H, NCH_2), 1.03 (d, *J* = 6.6 Hz, 6H, N(CH)-CH_3). **^{13}C NMR** (125 MHz, $CDCl_3$) δ (ppm) 156.35 (1C, CO) 69.30 (2C, OCH_2), 55.24 (1C, NCH), 50.63 (2C, NCH_2), 18.78 (2C, N(CH)-CH_3).

6-Butyl-1,3,6-dioxazocane (5d). **^{1}H NMR** (500 MHz, $CDCl_3$) δ (ppm) 4.18-4.20 (t, *J* = 5.4 Hz, 4H, OCH_2), 2.79-2.81 (t, *J* = 5.4 Hz, 4H, NCH_2), 2.60-2.64 (t, *J* = 7.2 Hz, 2H, $NC\underline{H}_2CH_2CH_2CH_3$), 1.41-1.47 (m, 2H, $NCH_2C\underline{H}_2CH_2CH_3$), 1.24-1.32 (m, 2H, $NCH_2CH_2C\underline{H}_2CH_3$), 0.89-0.92 (t, *J* = 7.4 Hz, 3H, CH_3). **^{13}C NMR** (125 MHz, $CDCl_3$) δ (ppm) 156.25 (1C, CO), 69.23 (2C, OCH_2), 56.83 (1C, $N\underline{C}H_2CH_2CH_2CH_3$), 54.21 (2C, NCH_2), 29.70 (1C, $NCH_2\underline{C}H_2CH_2CH_3$), 20.24 (1C, $NCH_2CH_2\underline{C}H_2CH_3$), 13.99 (1C, CH_3). **HR-MS (ESI)** m/z calculated for $C_9H_{18}NO_3$ ([M+H]+), **188.1281**, found, **188.1276**; Calculated for $C_9H_{18}NO_3$ ([M+Na]+), **210.1100**, found, **210.1091**.

6-(*sec*-Butyl)-1,3,6-dioxazocane (5e). **^{1}H NMR** (500 MHz, $CDCl_3$) δ (ppm) 4.19-4.21 (t, *J* = 5.0 Hz, 4H, OCH_2), 2.73-2.83 (m, 4H, NCH_2), 2.61-2.67 (m, 1H, $N(CH_3)C\underline{H}CH_2CH_3$), 1.23-1.34, 1.54-1.63, (m, 2H, $N(CH_3)CHC\underline{H}_2CH_3$), 1.02-1.03 (d, *J* = 6.6 Hz, 3H, $N(C\underline{H}_3)CHCH_2CH_3$), 0.89-0.92 (t, *J* = 7.4 Hz, 3H, $N(CH_3)CHCH_2C\underline{H}_3$). **^{13}C NMR** (125 MHz, $CDCl_3$) δ (ppm) 156.24 (1C, CO), 69.40 (2C, OCH_2), 62.15 (1C, $N(CH_3)\underline{C}HCH_2CH_3$), 51.16 (2C, NCH_2), 27.01 (1C, $N(CH_3)CH\underline{C}H_2CH_3$), 15.54 (1C, $N(\underline{C}H_3)CHCH_2CH_3$), 11.56 (1C, $N(CH_3)CHCH_2\underline{C}H_3$). **HR-MS (ESI)** m/z calculated for $C_9H_{18}NO_3$ ([M+H]+), **188.1281**, found, **188.127**4; Calculated for $C_9H_{18}NO_3$ ([M+Na]+), **210.1100**, found, **210.1095**.

6-(*iso*-Butyl)-1,3,6-dioxazocane (5f). **^{1}H NMR** (500 MHz, $CDCl_3$) δ (ppm) 4.18-4.20 (t, *J* = 5.4 Hz, 4H, OCH_2), 2.80-2.82 (t, *J* = 5.4 Hz, 4H, NCH_2), 2.40-2.41 (d, *J* = 7.2 Hz, 2H, $NC\underline{H}_2CH(CH_3)_2$), 1.67-1.75 (m, 1H, $NCH_2C\underline{H}(CH_3)_2$)), 0.88-0.89 (d, *J* = 6.6 Hz, 6H, $NCH_2CH(C\underline{H}_3)_2$)). **^{13}C NMR** (125 MHz, $CDCl_3$) δ (ppm) 156.09 (1C, CO), 69.33 (2C, OCH_2), 65.59 (1C, $N\underline{C}H_2CH(CH_3)_2$), 55.11 (2C, NCH_2), 27.57 (1C, $NCH_2\underline{C}H(CH_3)_2$), 20.59 (2C, $NCH_2CH(\underline{C}H_3)_2$). **HR-MS (ESI)** m/z calculated for $C_9H_{18}NO_3$ ([M+H]+), **188.1281**, found, **188.1284**.

6-(*tert*-Butyl)-1,3,6-dioxazocane (5g). **^{1}H NMR** (500 MHz, $CDCl_3$) δ (ppm) 4.18-4.20 (t, *J* = 5.4 Hz, 4H, OCH_2), 2.83 (br, 4H, NCH_2), 1.13 (s, 9H, CH_3). **^{13}C NMR** (125 MHz, $CDCl_3$) δ (ppm) 156.33 (1C, CO), 69.45 (2C, OCH_2), 55.45 (1C, $N\underline{C}(CH_3)_3$), 49.10 (2C, NCH_2), 26.86 (3C, $NC(\underline{C}H_3)_3$). **HR-MS (ESI)** m/z calculated for $C_9H_{18}NO_3$ ([M+H]+), **188.1281**, found, **188.1279**; Calculated for $C_9H_{18}NO_3$ ([M+Na]+), **210.1100**, found, **210.1104**.

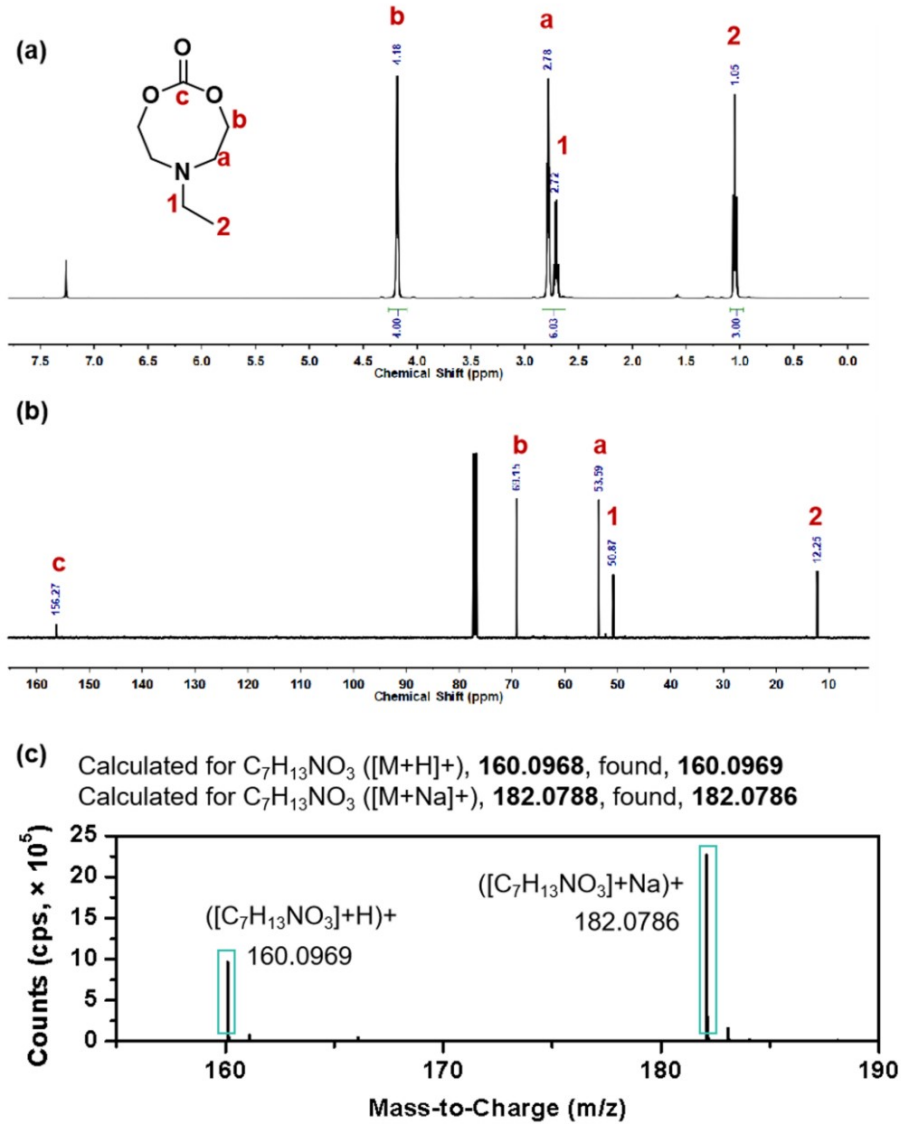

Figure S4. (a) ^{1}H NMR and (b) ^{13}C NMR spectra of 6-ethyl-1,3,6-dioxazocan-2-one **5a**.

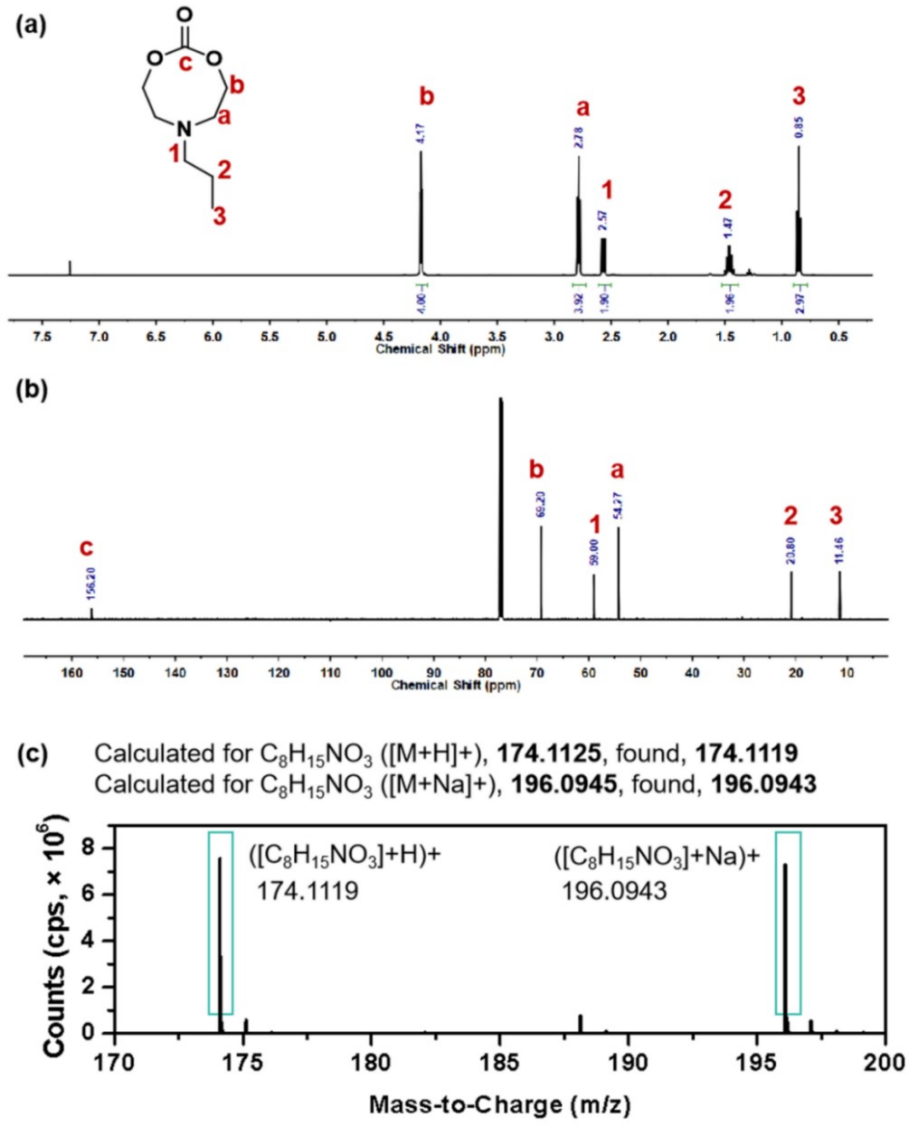

Figure S5. (a) ^{1}H NMR and (b) ^{13}C NMR spectra of 6-propyl-1,3,6-dioxazocan-2-one **5b**.

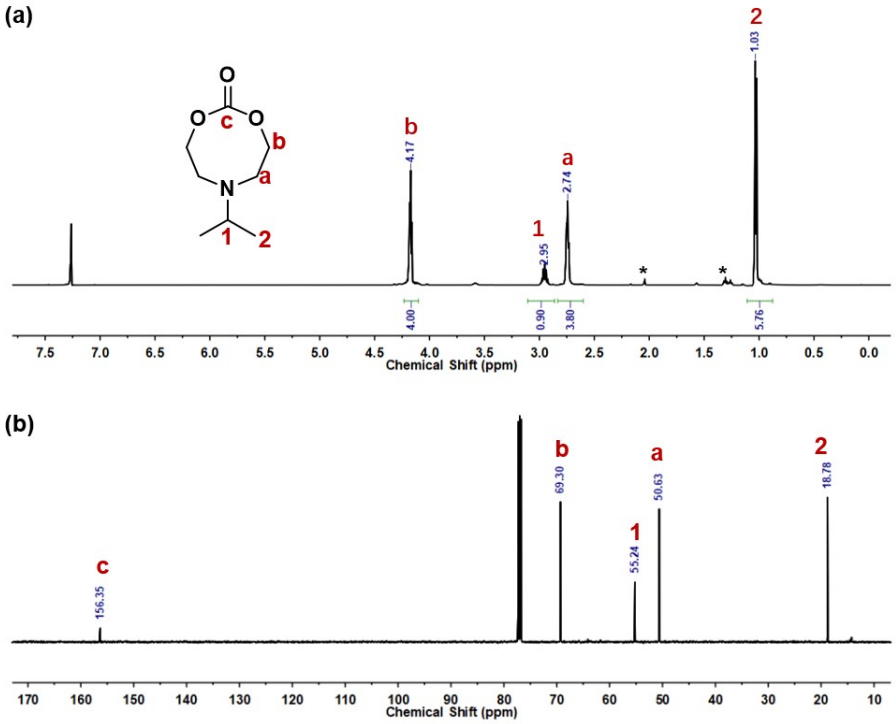

Figure S6. (a) ^{1}H NMR and (b) ^{13}C NMR spectra of *N-iso*-propyl-1,3,6-dioxazocane **5c**. The asterisk signals are related to ethyl acetate.

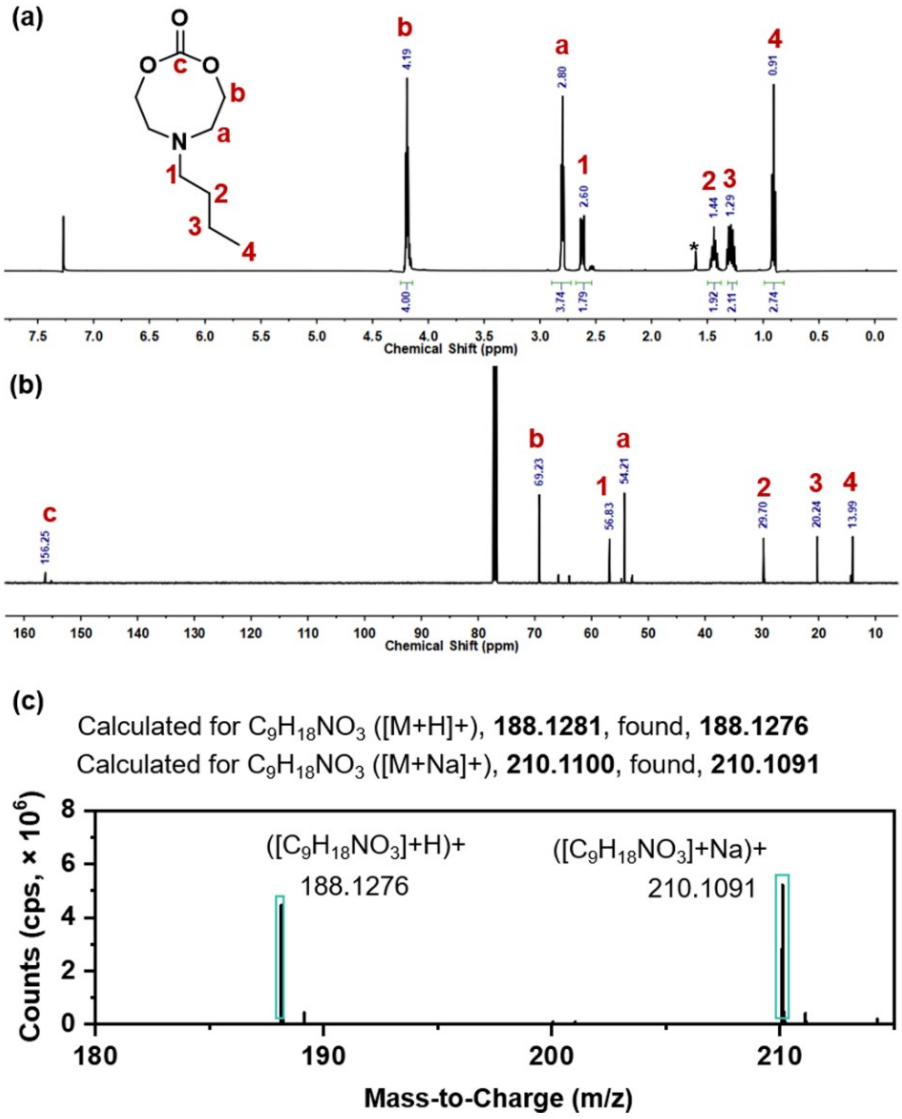

Figure S7. (a) ^{1}H NMR, (b) ^{13}C NMR and (c) HR-ESI-MS spectra of 6-butyl-1,3,6-dioxazocan-2-one **5d**. The asterisk signal is attributed to H_2O.

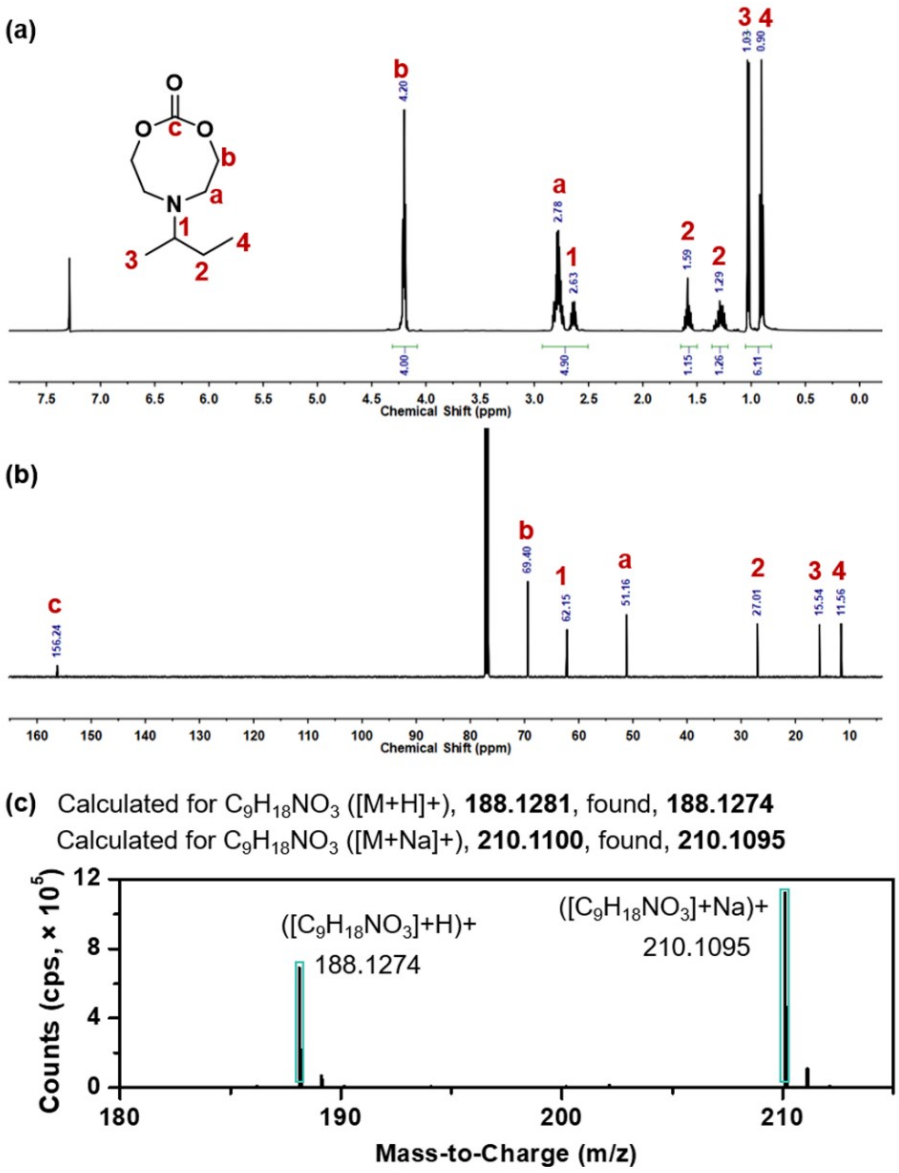

Figure S8. (a) ^{1}H NMR (b) ^{13}C NMR and (c) HR-ESI-MS spectra of 6-(*sec*-butyl)-1,3,6-dioxazocan-2-one **5e**.

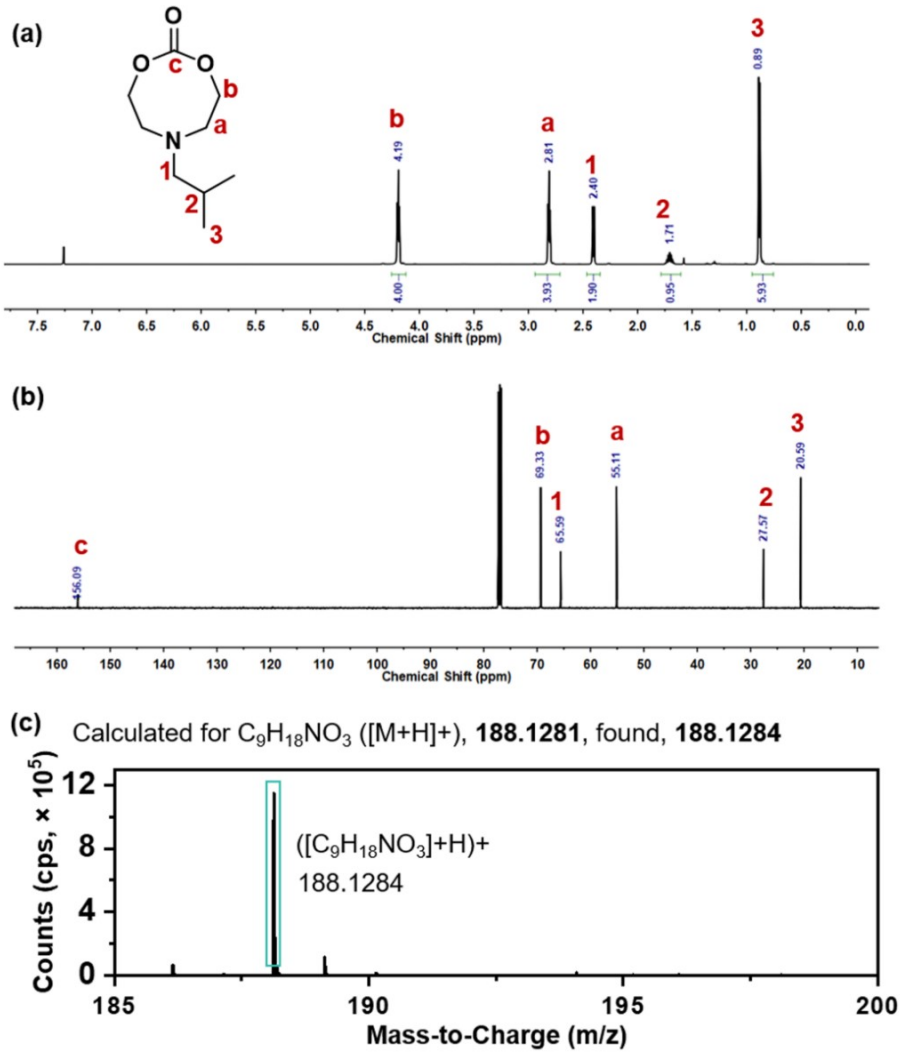

Figure S9. (a) ^{1}H NMR, (b) ^{13}C NMR and (c) HR-ESI-MS spectra of 6-(*iso*-butyl)-1,3,6-dioxazocan-2-one **5f**.

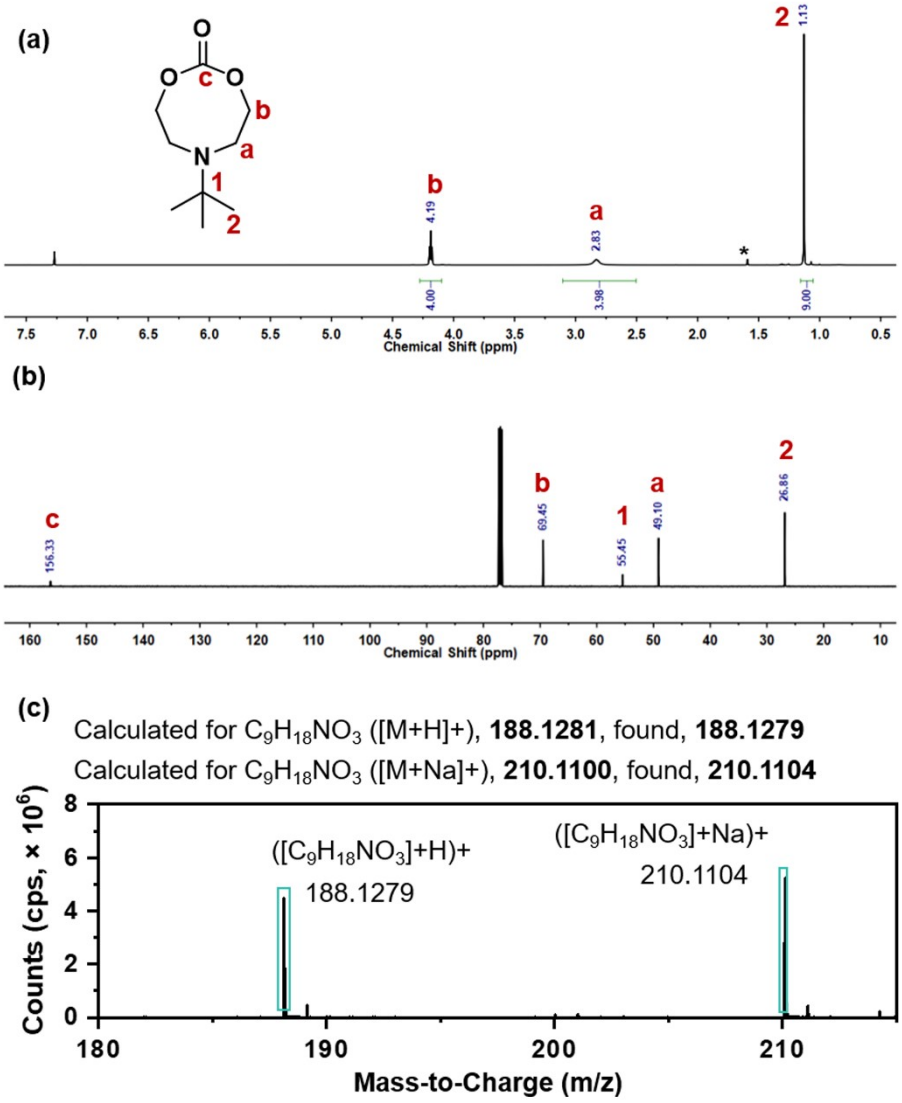

Figure S10. (a) ^{1}H NMR, (b) ^{13}C NMR and (c) HR-ESI-MS spectra of 6-(*tert*-butyl)-1,3,6-dioxazocan-2-one **5g**. The asterisk signal is attributed to H_2O.

2.6 Synthesis of Petasis reagent.

In a round-bottle flask, bis(cyclopentadienyl)titanium (IV)) dichloride (16.0 g, 64.3 mmol, 1.0 eq.) and 160 mL toluene were added and well mixed in a NaCl/ice bath. After stirring for 30 min, 50 mL MeMgCl in THF (150 mmol, 2.3 eq.) was added drop-wise in 30 min. The flask was kept around -10 ˚C and stirring for 1h. The viscous mixture was quenched with ice cold 6 % aq. NH_4Cl solution (2.8 g NH_4Cl/44 mL H_2O). The reaction mixture was stirred for another 1h and washed with 60 mL cold water for 3 times, followed by 60 mL cold saturated NaCl solution for 2 times. The orange organic phase was collected and dried with $NaSO_4$. The final weight percentage of Petasis reagent in toluene/THF was calculated using ^{1}H NMR spectrum.

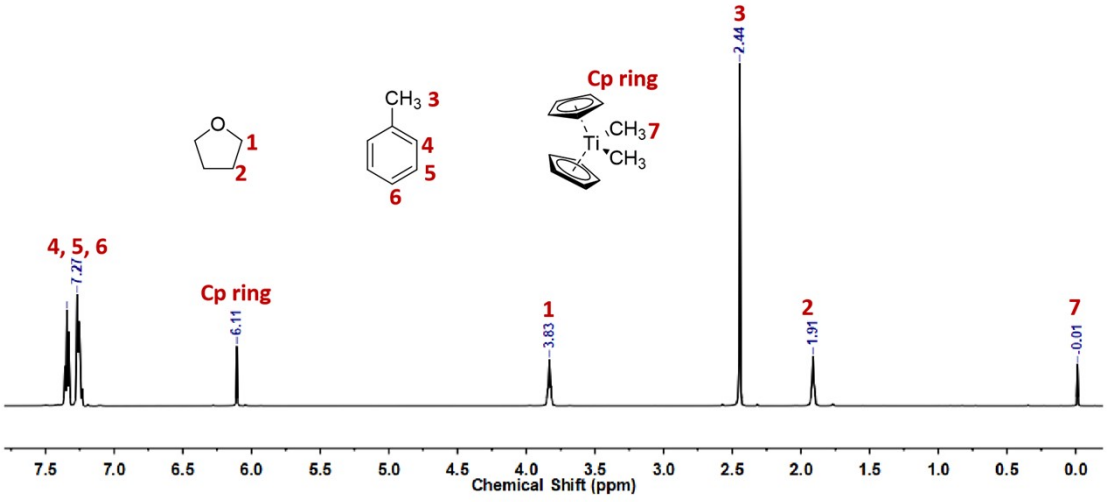

Figure S11. ^{1}H NMR spectrum of Petasis reagent.

2.7 Synthesis of Alkyl-substituted-2-methylene-1,3,6-dioxazocane **7a-g**

The intermediate cyclic carbonate (1.0 eq.), freshly prepared Petasis reagent (2.3 eq.) and anhydrous THF were charged into a round-bottom flask and heated up to 65 ˚C. After 22 h, 200 mL *n*-hexane was added into the flask. Yellow precipitation was afforded immediately. The precipitate was isolated using filtration paper and disposed. The solvent was removed using a rotary evaporator. The concentrated mixture was rediluted with *n*-hexane again and followed by the filtration step. Above steps were repeated few times until no precipitation can be found. After that, the concentrated viscous mixture was subjected to vacuum distillation in an oil bath. Under 10-15 mbar, 40-65 ˚C, dark yellow oily liquid was collected as aimed substance.

6-Ethyl-2-methylene-1,3,6-dioxazocane (7a). ^{1}H NMR (500 MHz, $CDCl_3$) δ (ppm) 4.00-4.02 (t, *J* = 5.0 Hz, 4H, OCH_2), 3.61 (s, 2H, CCH_2), 2.79-2.81 (t, *J* = 5.0 Hz, 4H, NCH_2), 2.65-2.69 (t, *J* = 7.0 Hz, 2H, NCH_2CH_3), 1.04-1.07 (t, *J* = 7.0 Hz, 3H, CH_3). **^{13}C NMR** (125 MHz, $CDCl_3$) δ (ppm) 163.77 (1C, $\underline{C}CH_2$), 70.06 (1C, $C\underline{C}H_2$), 69.78 (2C, OCH_2), 54.50 (2C, NCH_2), 50.42 (1C, $N\underline{C}H_2CH_3$), 12.54 (1C, $NCH_2\underline{C}H_3$). **HR-MS (ESI)** m/z calculated for $C_8H_{16}NO_2$ ([M+H]+), **158.1176**, found, **158.1178.**

6-Propyl-2-methylene-1,3,6-dioxazocane (7b). ^{1}H NMR (500 MHz, $CDCl_3$) δ (ppm) 3.98-4.00 (t, *J* = 5.4 Hz, 4H, OCH_2), 3.59 (s, 2H, CCH_2), 2.79-2.81 (t, *J* = 5.4 Hz, 4H, NCH_2), 2.53-2.55 (t, *J* = 7.2 Hz, 2H, $NC\underline{H}_2CH_2CH_3$), 1.42-1.50 (m, 2H, $NCH_2C\underline{H}_2CH_3$), 0.88-0.90 (t, *J* = 7.2 Hz, 3H, $NCH_2CH_2C\underline{H}_3$). **^{13}C NMR** (125 MHz, $CDCl_3$) δ (ppm) 162.99 (1C, $\underline{C}CH_2$), 68.82 (1C, $C\underline{C}H_2$), 68.71 (2C, OCH_2), 57.46 (1C, $N\underline{C}H_2CH_2CH_3$), 53.96 (2C, NCH_2), 19.84 (1C, $NCH_2\underline{C}H_2CH_3$), 10.64 (1C, $NCH_2CH_2\underline{C}H_3$). **HR-MS (ESI)** m/z calculated for $C_9H_{18}NO_2$ ([M+H]+), **172.1340**, found, **172.1334**.

6-(*iso*-Propyl)-2-methylene-1,3,6-dioxazocane (7c). ^{1}H NMR (500 MHz, $CDCl_3$) δ (ppm) 3.97-3.99 (t, *J* = 5.0 Hz, 4H, OCH_2), 3.56 (s, 2H, CCH_2), 2.90-2.98 (m, 1H, NCH), 2.70-2.72 (t, *J* = 5.4 Hz, 4H, NCH_2), 1.00 (d, *J* = 6.6 Hz, 6H, N(CH)-CH_3). **^{13}C NMR** (125 MHz, $CDCl_3$) δ (ppm) 164.58 (1C, CO) 71.01 (2C, OCH_2), 69.33 (1C, CCH_2), 55.16 (1C, NCH), 51.27 (2C, NCH_2), 18.54 (2C, N(CH)-CH_3).

6-Butyl-2-methylene-1,3,6-dioxazocane (7d). ^{1}H NMR (500 MHz, $CDCl_3$) δ (ppm) 3.99-4.01 (t, *J* = 5.0 Hz, 4H, OCH_2), 3.60 (s, 2H, CCH_2), 2.79-2.81 (t, *J* = 4.8 Hz, 4H, NCH_2), 2.56-2.59 (t, *J* = 7.2 Hz, 2H, $NC\underline{H}_2CH_2CH_2CH_3$), 1.38-1.47 (m, 2H, $NCH_2C\underline{H}_2CH_2CH_3$), 1.28-1.36 (m, 2H, $NCH_2CH_2C\underline{H}_2CH_3$), 0.89-0.92 (t, *J* = 7.2 Hz, 3H, $NCH_2CH_2CH_2C\underline{H}_3$). **^{13}C NMR** (125 MHz, $CDCl_3$) δ (ppm) 164.11 (1C, CO), 70.02 (1C, CCH_2), 69.88 (2C, OCH_2), 56.36 (1C, $N\underline{C}H_2CH_2CH_2CH_3$), 55.14 (2C, NCH_2), 30.00 (1C, $NCH_2\underline{C}H_2CH_2CH_3$), 20.52 (1C, $NCH_2CH_2\underline{C}H_2CH_3$), 14.13 (1C, $NCH_2CH_2CH_2\underline{C}H_3$). **HR-MS (ESI)** m/z calculated for $C_{10}H_{20}NO_2$ ([M+H]+), **186.1489**, found, **186.1483**.

6-(*sec*-Butyl)-2-methylene-1,3,6-dioxazocane (7e). **^{1}H NMR** (500 MHz, $CDCl_3$) δ (ppm) 3.97-3.99 (t, *J* = 5.0 Hz, 4H, OCH_2), 3.55 (s, 2H, CCH_2), 2.73-2.77, 2.63-2.68 (t, 4H, NCH_2), 2.54-2.61 (m, 1H, $N(CH_3)C\underline{H}CH_2CH_3$), 1.42-1.50, 1.20-1.29, (m, 2H, $N(CH_3)CHC\underline{H}_2CH_3$), 0.93-0.95 (d, *J* = 6.6 Hz, 3H, $N(C\underline{H}_3)CHCH_2CH_3$), 0.89-0.92 (t, *J* = 7.2 Hz, 3H, $N(CH_3)CHCH_2C\underline{H}_3$). **^{13}C NMR** (125 MHz, $CDCl_3$) δ (ppm) 164.82 (1C, CO), 70.88 (2C, OCH_2), 69.01 (1C, CCH_2), 62.17 (1C, $N(CH_3)\underline{C}HCH_2CH_3$), 51.40 (2C, $N\underline{C}H_2$), 27.24 (1C, $N(CH_3)CH\underline{C}H_2CH_3$), 14.69 (1C, $N(\underline{C}H_3)CHCH_2CH_3$), 11.61 (1C, $N(CH_3)CHCH_2\underline{C}H_3$). **HR-MS (ESI)** *m/z* calculated for $C_{10}H_{20}NO_2$ ($[M+H]^+$), **186.1489**, found, **186.1491**.

6-(i*so*-Butyl)-2-methylene-1,3,6-dioxazocane (7f). **^{1}H NMR** (500 MHz, $CDCl_3$) δ (ppm) 3.98-4.00 (t, *J* = 4.8 Hz, 4H, OCH_2), 3.58 (s, 2H, CCH_2), 2.77-2.79 (t, *J* = 4.8 Hz, 4H, NCH2), 2.35-2.37 (d, *J* = 7.2 Hz, 2H, $NC\underline{H}_2CH(CH_3)_2$)), 1.60-1.68 (m, 1H, $NCH_2C\underline{H}(CH_3)_2$)), 0.88-0.89 (d, *J* = 6.6 Hz, 6H, $NCH_2CH(C\underline{H}_3)_2$)). **^{13}C NMR** (125 MHz, $CDCl_3$) δ (ppm) 164.30 (1C, CO), 69.66 (2C, OCH_2), 69.49 (1C, CCH_2), 65.00 (1C, $N\underline{C}H_2CH(CH_3)_2$), 55.49 (2C, NCH_2), 26.99 (1C, $NCH_2\underline{C}H(CH_3)_2$), 20.57 (2C, $NCH_2CH(\underline{C}H_3)_2$). **HR-MS (ESI)** m/z calculated for $C_{10}H_{20}NO_2$ ([M+H]+), **186.1489**, found, **186.1491**.

6-(*tert*-Butyl)-2-methylene-1,3,6-dioxazocane (7g). **^{1}H NMR** (500 MHz, $CDCl_3$) δ (ppm) 3.95-3.98 (t, *J* = 4.8 Hz, 4H, OCH_2), 3.53 (s, 2H, CCH_2), 2.74-2.77 (t, *J* = 5.0 Hz, 4H, NCH_2), 1.06 (s, 9H, CH_3). **^{13}C NMR** (125 MHz, $CDCl_3$) δ (ppm) 165.09 (1C, CO), 71.63 (2C, OCH_2), 69.24 (1C, CCH_2), 55.03 (1C, $N\underline{C}(CH_3)_3$), 49.36 (2C, NCH_2), 26.92 (3C, $NC(\underline{C}H_3)_3$). **HR-MS (ESI)** m/z calculated for $C_{10}H_{20}NO_2$ ([M+H]+), **186.1489**, found, **152.1470**.

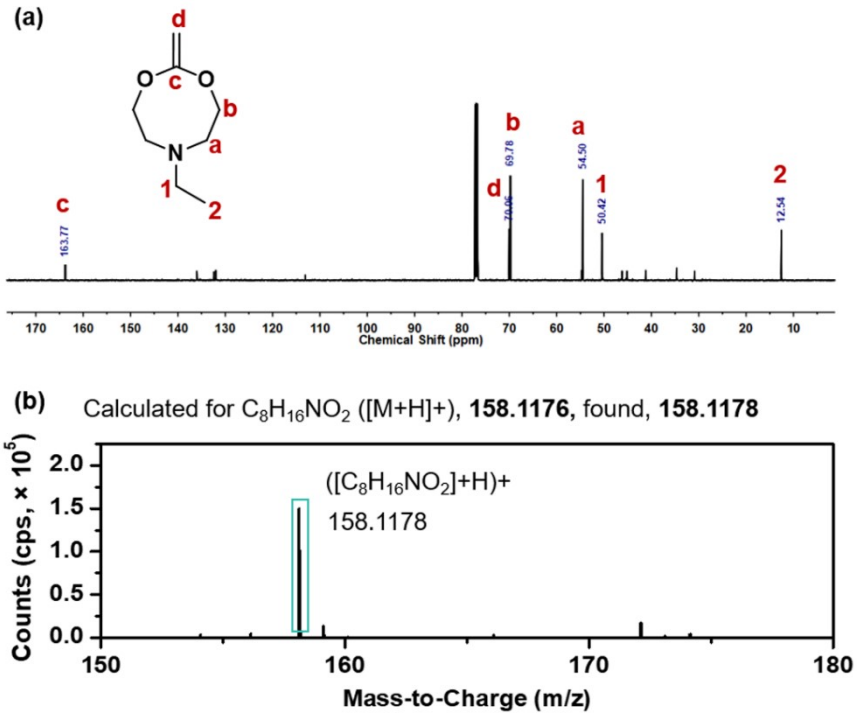

Figure S12. (a) ^{13}C NMR and (b) HR-ESI-MS spectra of 6-ethyl-2-methylene-1,3,6-dioxazocane **7a**.

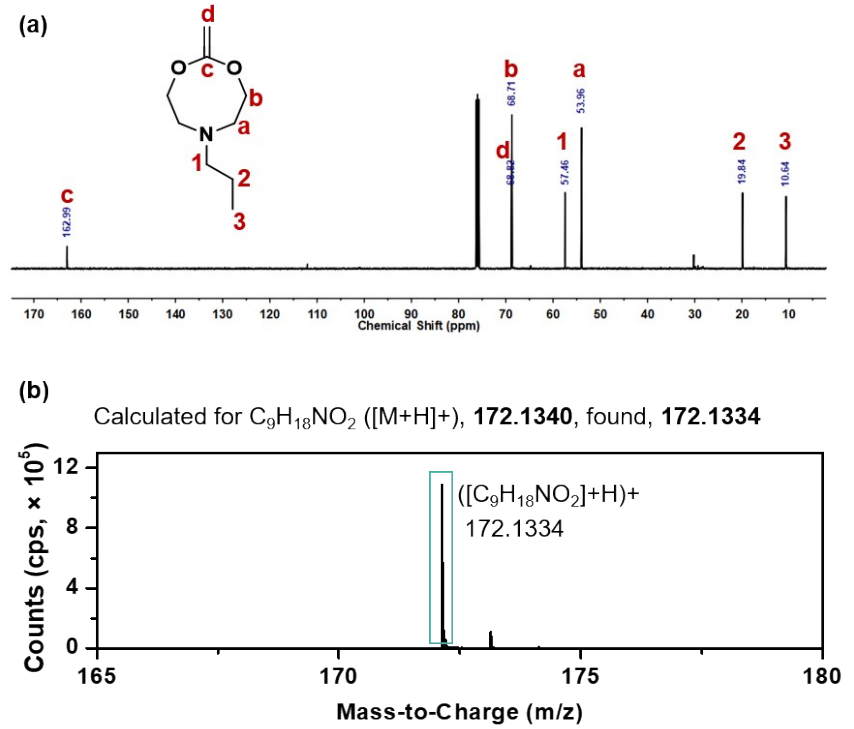

Figure S13. (a) ^{13}C NMR and (b) HR-ESI-MS spectra of 6-Propyl-2-methylene-1,3,6-dioxazocane **7b**.

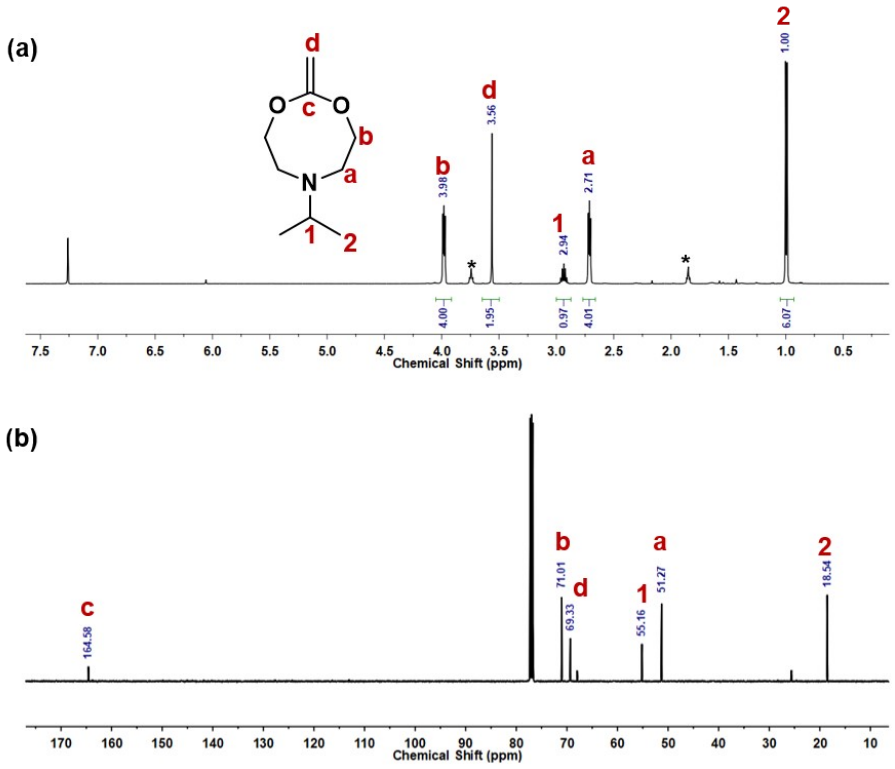

Figure S14. (a) ^{1}H NMR and (b) ^{13}C NMR spectra of *N-iso*-propyl-2-methylene-1,3,6-dioxazocane **7c**. The asterisk signals are related to THF.

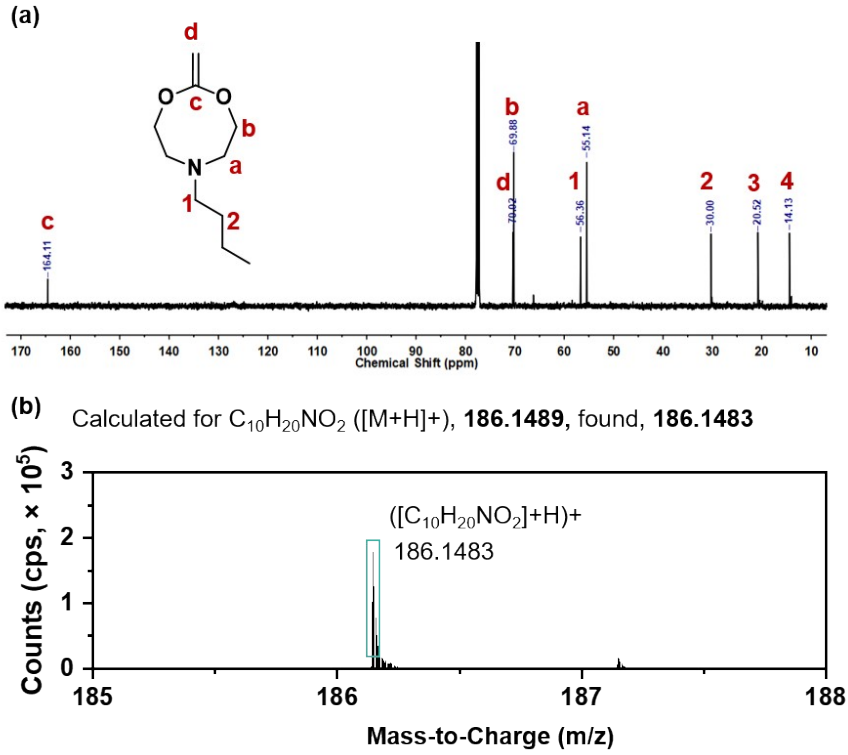

Figure S15. (a) ^{1}H NMR, (b) ^{13}C NMR and (c) HR-ESI-MS spectra of 6-butyl-2-methylene-1,3,6-dioxazocane **7d**.

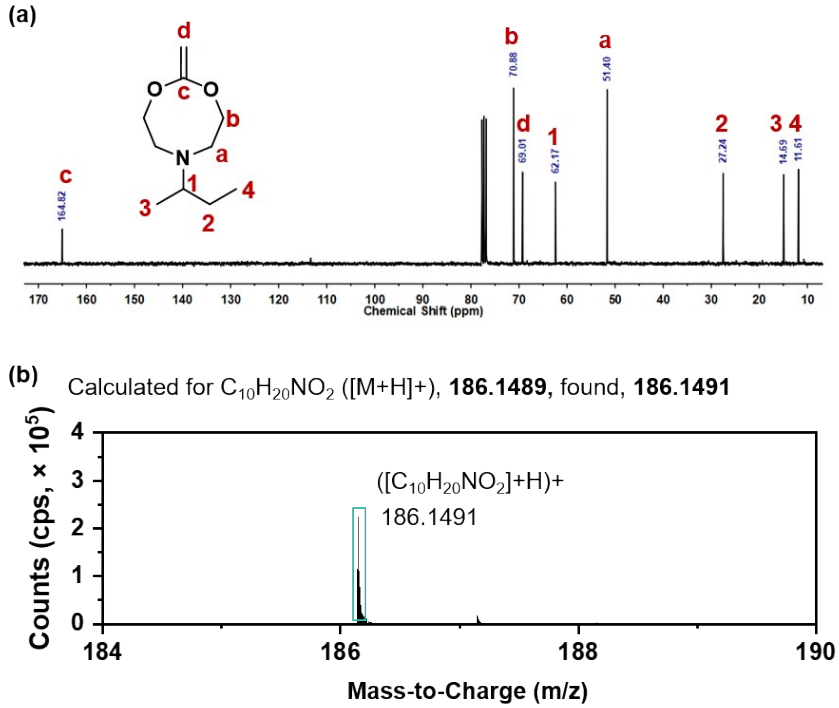

Figure S16. (a) ^{13}C NMR and (b) HR-ESI-MS spectra of 6-(*sec*-butyl)-2-methylene-1,3,6-dioxazocane **7e**.

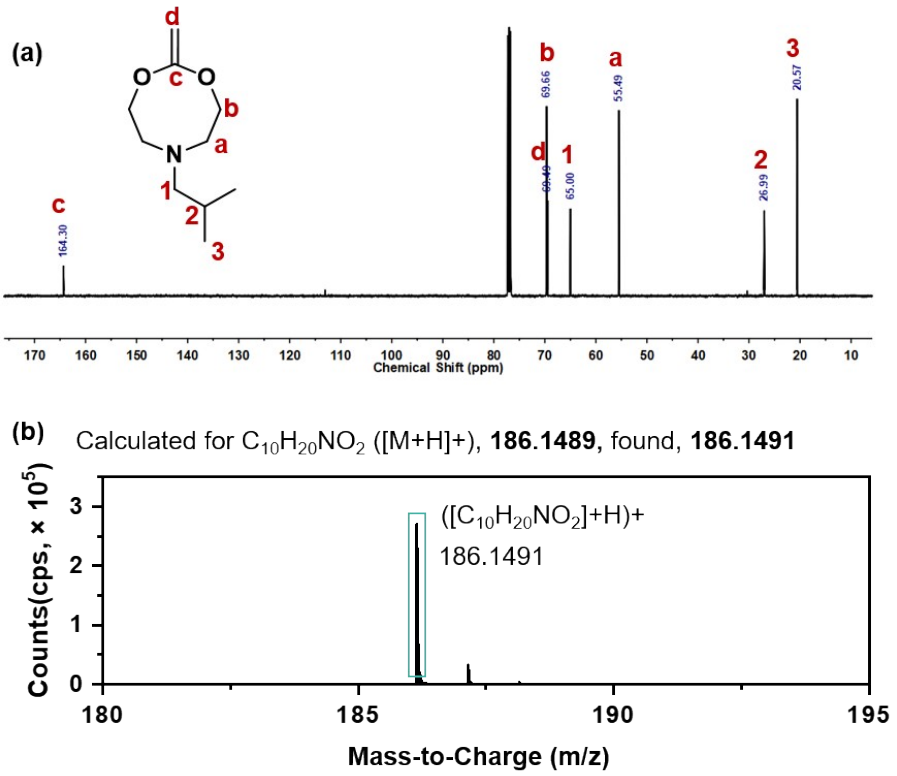

Figure S17. (a) ^{13}C NMR and (b) HR-ESI-MS spectra of 6-(*iso*-butyl)-2-methylene-1,3,6-dioxazocane **7f**.

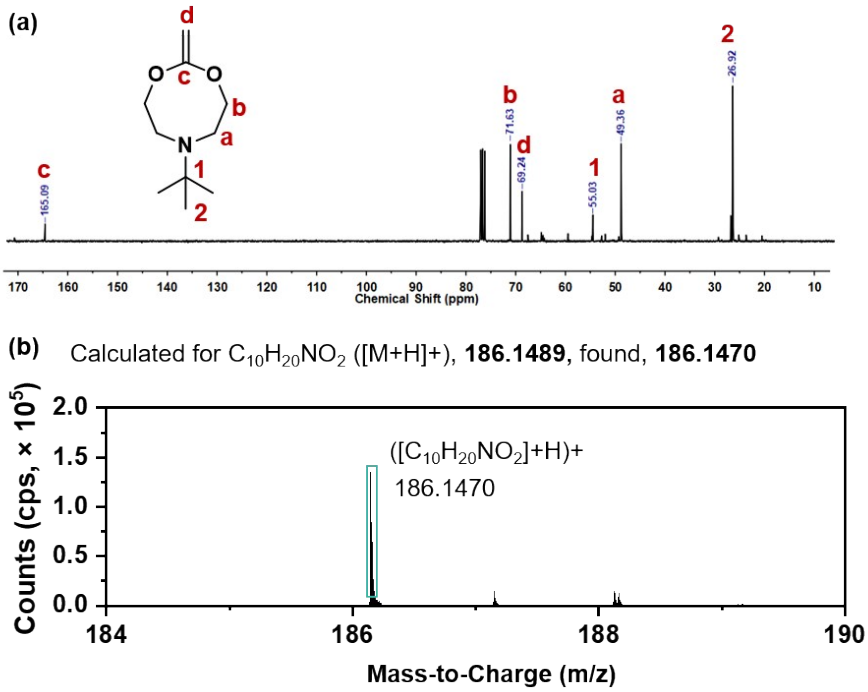

Figure S18. (a) ^{13}C NMR and (b) HR-ESI-MS spectra of 6-(*tert*-butyl)-2-methylene-1,3,6-dioxazocane **7g**.

Table S1. Yield of Alk-MACs **7a-g**

MAC	Carbonate (eq.)	Petasis reagent (eq.)	Temperature (°C)	Reaction duration (h)	Yield (%)
7a	1.0	2.3	65	22	12
7b	1.0	2.3	65	22	12
7c	1.0	2.3	65	22	25[a]
7d	1.0	2.3	65	22	6
7e	1.0	2.3	65	22	15
7f	1.0	2.3	65	22	11
7g	1.0	2.3	65	22	15

[a]According to the reported work, **7c** was obtained in a yield of 11%. Here we adopted similar synthetic method and achieved a higher yield of 25%.

2.8 2D NMR spectra of *sec*-butyl-derivatives and *iso*-propyl-derivatives

Signals of the protons **a**, **a'** and **2**, **2'** of the chiral ^{s}Bu-MAC **7e** and the corresponding carbonate **5e** showed an additional splitting (see in Fig. 2 and S8). HSQC NMR techniques for **7e** and **5e** showed different chemical shifts of the diastereotopic protons **2** (Fig. S19), which is typical for chiral molecules. Also, as diastereotopic protons, protons **a** are split, but much less than protons **2** as they are further away from the chiral centre. No further diastomeric signal splitting could be detected with the 500 MHz setup used in here.

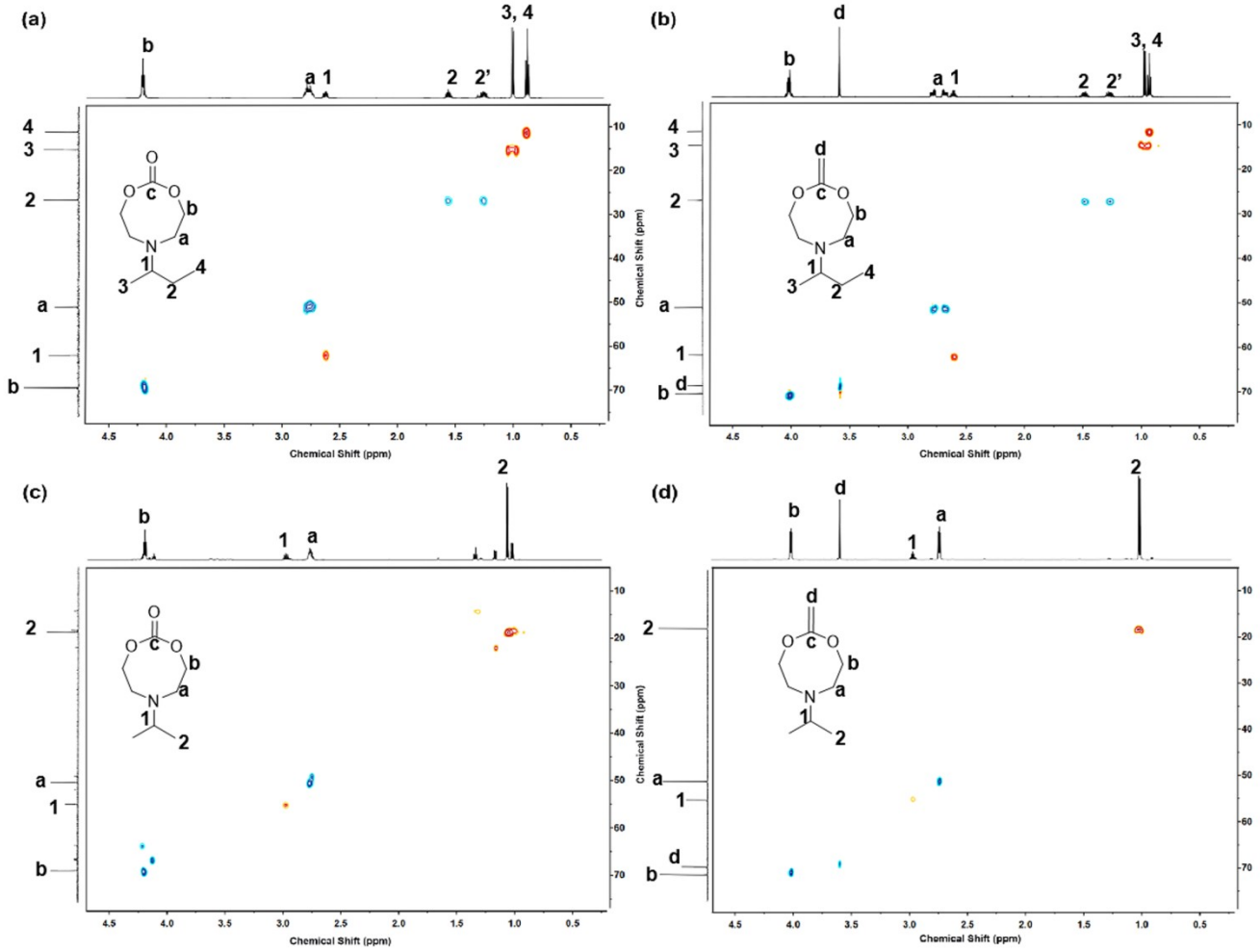

Figure S19. 2D HSQC NMR spectra of (a) ^{s}Bu-cyclic carbonate, (b) ^{s}Bu-MAC (c) ^{i}Pr-cyclic carbonate and (d) ^{i}Pr-MAC.

2.9 Optimization of alkyl-substituted diethanolamine preparation

Table S2. Yield of *N*-propyldiethanolamine **3b** prepared under different conditions

Entry	Diethanolamine (eq.)	1-Bromopropane (eq.)	Temperature (°C)	Reaction duration (h)	Yield (%)
1	1.0	1.0	65	72	72
2	1.0	1.0	65	84	60
3	1.0	1.0	65	96	44
4	1.0	1.0	75	72	35

Table S3. Yield of *N-iso*-propyldiethanolamine **3c** prepared under different conditions

Entry	Diethanolamine (eq.)	1-Bromopropane (eq.)	Temperature (°C)	Reaction duration (h)	Yield (%)
1	1.0	1.0	65	96	45
2	1.0	1.0	65	120	50
3	1.0	1.0	65	144	56
4	1.0	1.0	75	96	50

Table S4. Yield of *sec*-butyldiethanolamine **3e** prepared under different conditions

Entry	Diethanolamine (eq.)	2-Bromobutane (eq.)	Temperature (°C)	Reaction duration (h)	Yield (%)
1	1.0	1.0	65	72	3
2	1.0	1.0	65	120	6
3	1.0	1.0	80	72	9
4	1.0	1.0	90	72	25
5	1.0	1.0	100	72	11

Table S5. Yield of *iso*-butyldiethanolamine **3f** prepared under different conditions

Entry	Diethanolamine (eq.)	2-Methyl-1-bromopropane (eq.)	Temperature (°C)	Reaction duration (h)	Yield (%)
1	1.0	1.0	65	24	30
2	1.0	1.0	75	6	9
3	1.0	1.0	75	24	34
4	1.0	1.0	75	120	< 1
5	1.0	1.0	90	24	< 1

2.10 Optimization of intermediate carbonate preparation

Table S6. Yield of 6-ethyl-1,3,6-dioxazocane **5a** prepared under different conditions

Entry	Diol (eq.)	Ethyl chloroformate (eq.)	TEA (eq.)	Feeding speed of TEA (µL/min)	Temperature (°C)	Reaction duration (h)	Yield (%)
1	1.0	6.2	4.0	200	0	20	0
2	1.0	6.2	4.0	15	0	20	5
3	1.0	6.2	4.0	15	-20	20	11
4	1.0	6.2	4.0	15	-78	110	-
5	1.0	6.2	4.0	15	-20	36	11
6	1.0	6.2	2.5	15	-20	36	16
7	1.0	6.2	1.5	15	-20	36	4
8	1.0	3.7	2.5	15	-20	36	9
9	1.0	2.5	2.5	15	-20	36	18
10	1.0	2.0	2.5	15	-20	36	23
11	1.0	1.5	2.5	15	-20	36	-

Table S7. Yield of 6-propyl-1,3,6-dioxazocane **5b** prepared under different conditions

Entry	Diol (eq.)	Ethyl chloroformate (eq.)	TEA (eq.)	Feeding speed of TEA (µL/min)	Temperature (°C)	Reaction duration (h)	Yield (%)
1	1.0	4.0	4.0	400	0	36	14
2	1.0	4.0	4.0	200	0	36	20
3	1.0	4.0	4.0	100	0	36	8
4	1.0	4.0	4.0	40	0	36	29
5	1.0	4.0	4.0	20	0	36	10

Table S8. Yield of 6-butyl-2-methylene-1,3,6-dioxazocane **5d** prepared under different conditions

Entry	Diol (eq.)	Ethyl chloroformate (eq.)	TEA (eq.)	Feeding speed of TEA (µL/min)	Temperature (°C)	Reaction duration (h)	Yield (%)
1	1.0	4.0	4.0	400	0	36	25
2	1.0	4.0	4.0	200	0	36	23
3	1.0	4.0	4.0	20	0	36	impure

Table S9. Yield of 6-(*sec*-butyl)-1,3,6-dioxazocane **5e** prepared under different conditions

Entry	Diol (eq.)	Ethyl chloroformate (eq.)	TEA (eq.)	Feeding speed of TEA (μL/min)	Temperature (°C)	Reaction duration (h)	Yield (%)
1	1.0	4.0	4.0	200	0	36	impure
2	1.0	4.0	4.0	100	0	36	45
3	1.0	4.0	4.0	50	0	36	40
4	1.0	4.0	4.0	20	0	36	41

Table S10. Yield of 6-(*iso*-butyl)-1,3,6-dioxazocane **5f** prepared under different conditions

Entry	Diol (eq.)	Ethyl chloroformate (eq.)	TEA (eq.)	Feeding speed of TEA (μL/min)	Temperature (°C)	Reaction duration (h)	Yield (%)
1	1.0	8.0	4.0	400	0	28	44
2	1.0	6.2	4.0	400	0	28	6
3	1.0	4.0	4.0	400	0	28	28
4	1.0	4.0	4.0	200	0	28	32
5	1.0	4.0	4.0	100	0	28	18

Table S11. Yield of 6-(*tert*-butyl)-1,3,6-dioxazocane **5g** prepared under different conditions

Entry	Diol (eq.)	Ethyl chloroformate (eq.)	TEA (eq.)	Feeding speed of TEA (μL/min)	Temperature (°C)	Reaction duration (h)	Yield (%)
1	1.0	4.0	4.0	200	0	36	impure
2	1.0	4.0	4.0	40	0	36	29
3	1.0	4.0	4.0	20	0	36	29

2.11 Theoretical calculation of Alk-MACs with the corresponding cyclic carbonate

The optimal theoretical calculations were performed using the software package GAMESS with the basis set STO-6G for all the molecules.[1]

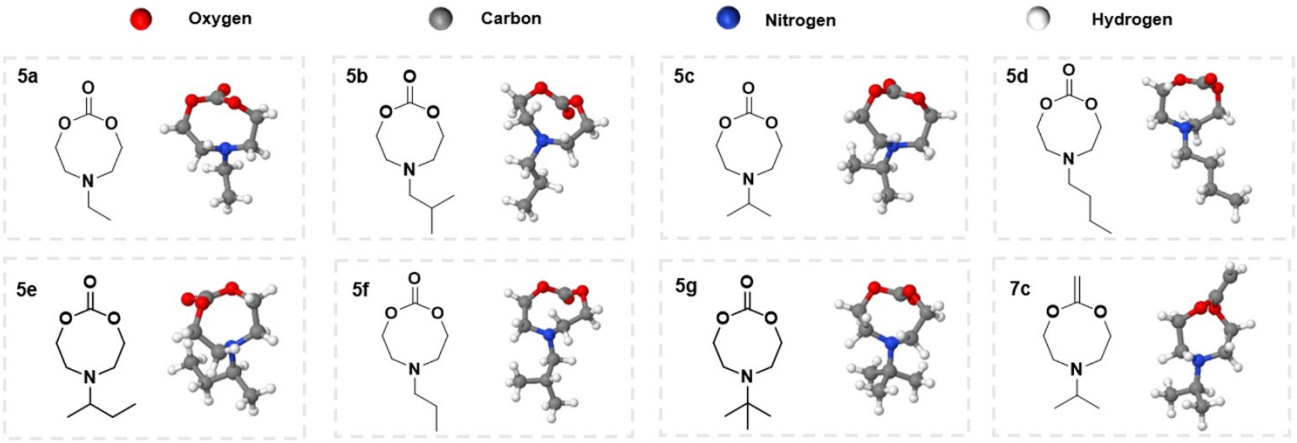

Figure S20. Optimal energetic structures of intermediate carbonate **5a-g** and Alk-MACs **7c** calculated at 0 K, under vacuum. Red balls represent oxygen atoms, grey balls represent carbon atoms, blue balls represent nitrogen atoms and white balls represent hydrogen atoms. The results of the remaining CKAs **7a-b** and **7d-g** have been shown in the main paper.

3 Poly(Alk-MAC-co-MTC) preparation and characterization

3.1 Copolymerization of Alk-MACs and MTC

In a SEC vial, Alk-MAC, MTC, initiator and a small stir bar were added to perform copolymerization. The composition of poly(^{i}Pr-MAC-co-MTC) was tuned with different ^{i}Pr-MAC **7c** to MTC molar ratio (5/95, 10/90, 25/75 and 50/50). AIBN (0.5 mol%) was used as thermal initiator and Irgacure 184 (0.5 mol%) was used as photo initiator. The reaction mixture was flushed with argon for 20 min and then heated up to 85 °C or exposed under UV light (365 nm) for 24 h. After polymerization, the reaction mixture became viscous and the color became darker. Diluted with some chloroform, the crude product was purified through dialysis in chloroform for 4 times and RC dialysis membrane was utilized for purification (MWCO: 1 k). Then the purified polymer was collected under reduced pressure. Other Alk-MACs were also copolymerized with MTC through thermal polymerization with a feed ratio of Alk-MAC/MTC = 25/75. The copolymerization method followed a similar way.

To make it brief, the samples were named according to the proportion of Alk-MAC and the polymerization method. For example, in ^{i}Pr-MAC-5T the number 5 stands for 5 mol% of **7c** and the letter T stands for the thermal polymerization. In the same way the letter U stands for the UV polymerization.

3.2 Conversion of ^{i}Pr-MAC **7c** and MTC

Poly(^{i}Pr-MAC-co-MTC) with various ^{i}Pr-MAC/MTC feed ratio were prepared by thermal and UV-irradiated polymerization. ^{i}Pr-MAC-25T is taken as an example here:

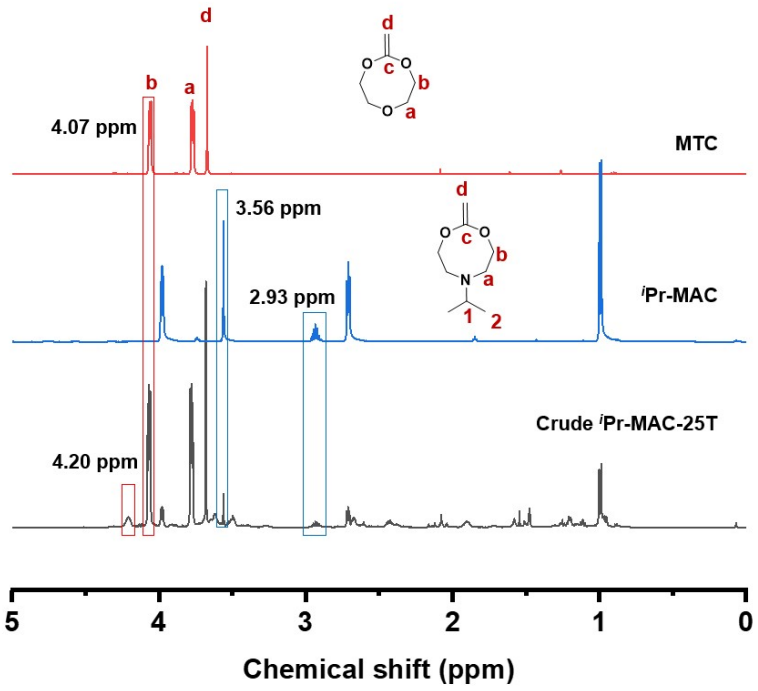

Figure S21. ^{1}H NMR spectra of MTC, ^{i}Pr-MAC **7c** and ^{i}Pr-MAC-25T crude product.

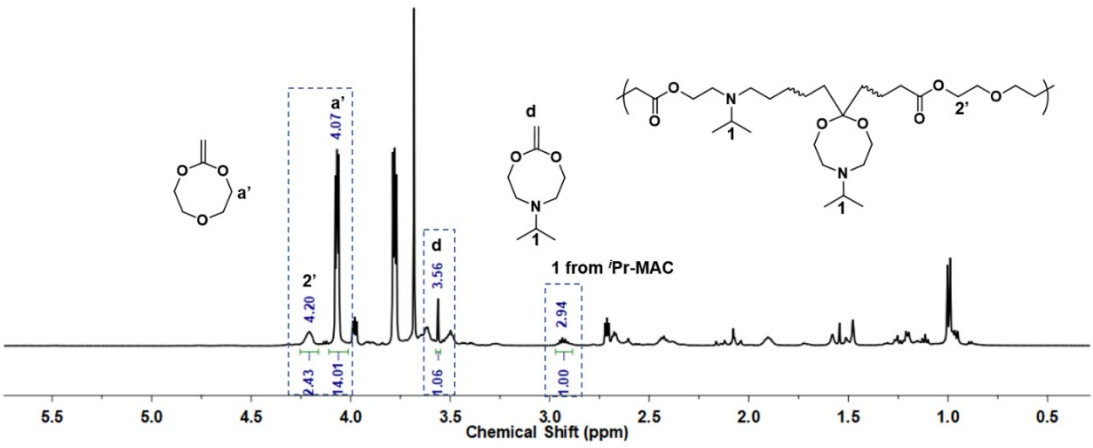

Figure S22. ^{1}H NMR spectrum of ^{i}Pr-MAC-25T crude product.

As reported in the literature, signal at 4.20 ppm is attributed to protons **2'** of P(MTC).[3] According to Figure S21, signal at 4.07 ppm (m, 4H, OCH_2) was taken as a reference for MTC monomer. The conversion of MTC was calculated with the following formula:

$$\text{conversion MTC} = \frac{\text{I(4.20 ppm)}}{\frac{\text{I(4.07 ppm)}}{2} + \text{I(4.20 ppm)}} \times 100\%$$

In Figure S22, signal at 2.93-2.94 ppm (m, 1H, NCH) represented the overlap of proton **1** of both ^{i}Pr-MAC **7c** and poly(^{i}Pr-MAC) segments. Signal at 3.56 ppm (s, 2H, CCH_2), attributed to the protons of double bond, can be used as a reference for **7c**. The conversion was calculated as follows:

$$\text{conversion } i\text{Pr - MAC} = \left(1 - \frac{\text{I(3.56 ppm)}}{2 \times \text{I(2.93 ppm)}}\right) \times 100\%$$

In Figure S22, conversion of MTC and ^{i}Pr-MAC **7c** was calculated for 26 and 47% respectively.

All the conversion of MTC/**7c** was calculated and recorded in **Table 1** in the main text.

3.3 Final molar fraction of ^{i}Pr-MAC **7c** and MTC

Purified ^{i}Pr-MAC-25T is taken as an example here:

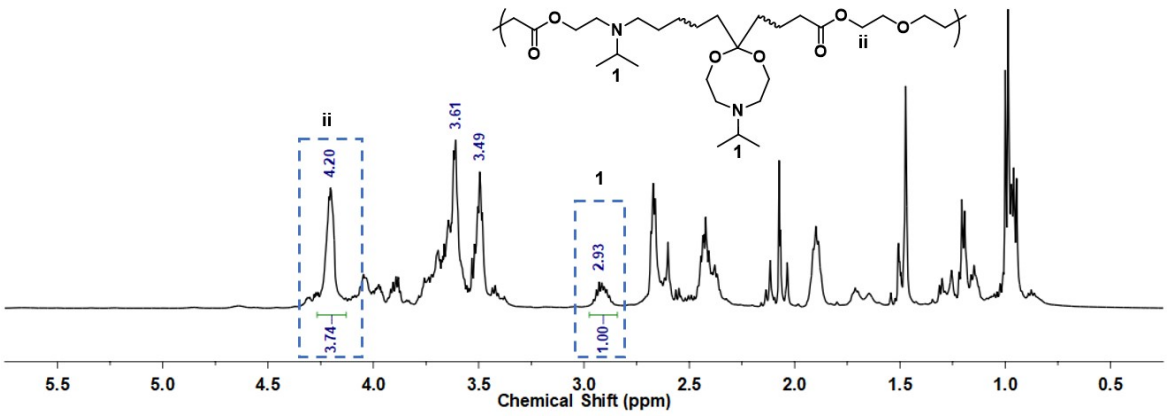

Figure S23. ^{1}H NMR spectrum of purified ^{i}Pr-MAC-25T.

Signal at 4.20 ppm was used as a reference for MTC moiety. Signal at 2.94 ppm was taken as a reference for ^{i}Pr-MAC **7c**. Final molar fraction of **7c** was calculated with the following formula:

$$F\mathbf{7c} = \frac{\mathrm{I}(2.93\ \mathrm{ppm})}{\frac{\mathrm{I}(4.20\ \mathrm{ppm})}{2} + \mathrm{I}(2.93\ \mathrm{ppm})} \times 100\%$$

$$F(\mathrm{MTC}) = 100\% - F(i\mathrm{Pr\text{-}MAC})$$

In Figure S23, final molar fraction of MTC and ^{i}Pr-MAC **7c** was calculated for 65 and 35% respectively.

All the final molar fraction value of MTC/**7c** was calculated and recorded in **Table 1** in the main text.

3.4 ^{1}H NMR spectra of P(^{i}Pr-MAC-co-MTC) copolymers

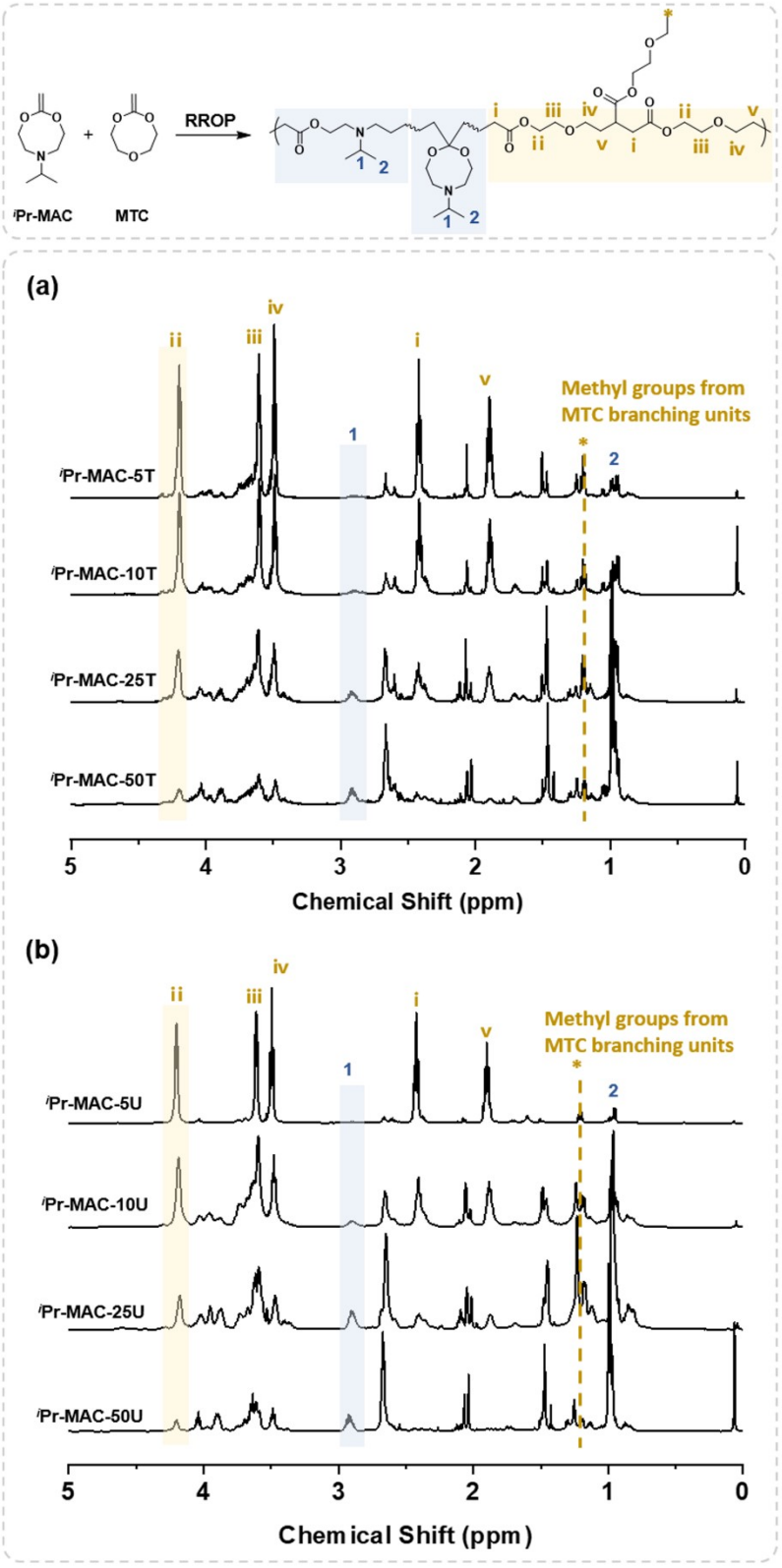

Figure S24. ^{1}H NMR spectra of P(^{i}Pr-MAC-co-MTC) copolymers prepared through thermal and UV-irradiated polymerization. * methyl group from the terminal of each MTC branching units, caused by MTC backbiting.[4]

3.5 ^{13}C NMR spectra of P(^{i}Pr-MAC-co-MTC) copolymers

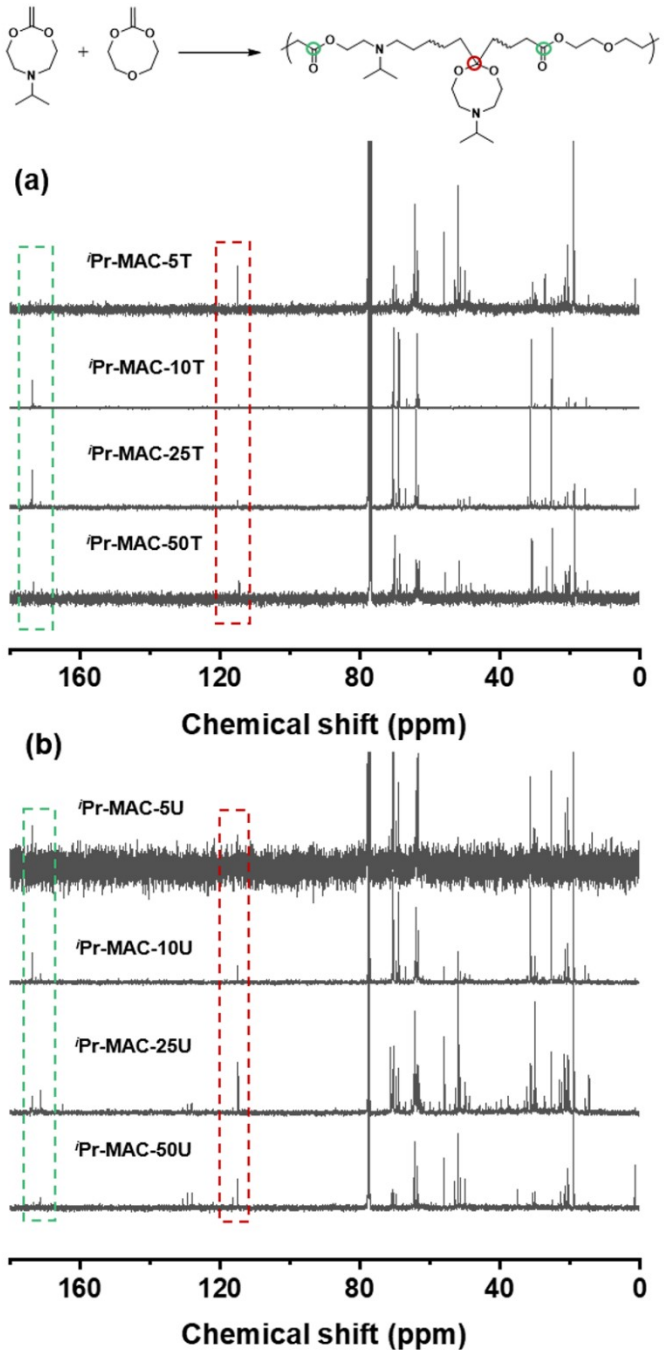

Figure S25. ^{13}C NMR spectra of P(^{i}Pr-MAC-co-MTC) copolymers prepared through thermal and UV-irradiated polymerization. Signals at 170-173.6 ppm are attributed to the carbonyl of ester units of ring-opening structure and signals around 114.6 ppm are related to the acetal of ring-retaining units.[2]

3.6 DOSY measurement of P(*i*Pr-MAC-co-MTC)

To confirm the formation of a copolymer rather than the simple mixture of PMTC and P(*i*Pr-MAC) homopolymers, a DOSY measurement of *i*Pr-MAC-5T was carried out. This sample was chosen as it showed a bimodal SEC trace in the RI-signal (see Figure S29). Self-diffusion coefficients of the P(*i*Pr-MAC)/PMTC segments are compared on the basis of the ^{1}H NMR spectrum. As shown in Figure S26, the self-diffusion coefficients related to tertiary amine groups (proton **1**) of P(*i*Pr-MAC) and protons **ii** of PMTC are in the range of the main diffusion signal (broad signal marked with red dashed line), therefore substantiating the presence of a copolymer.

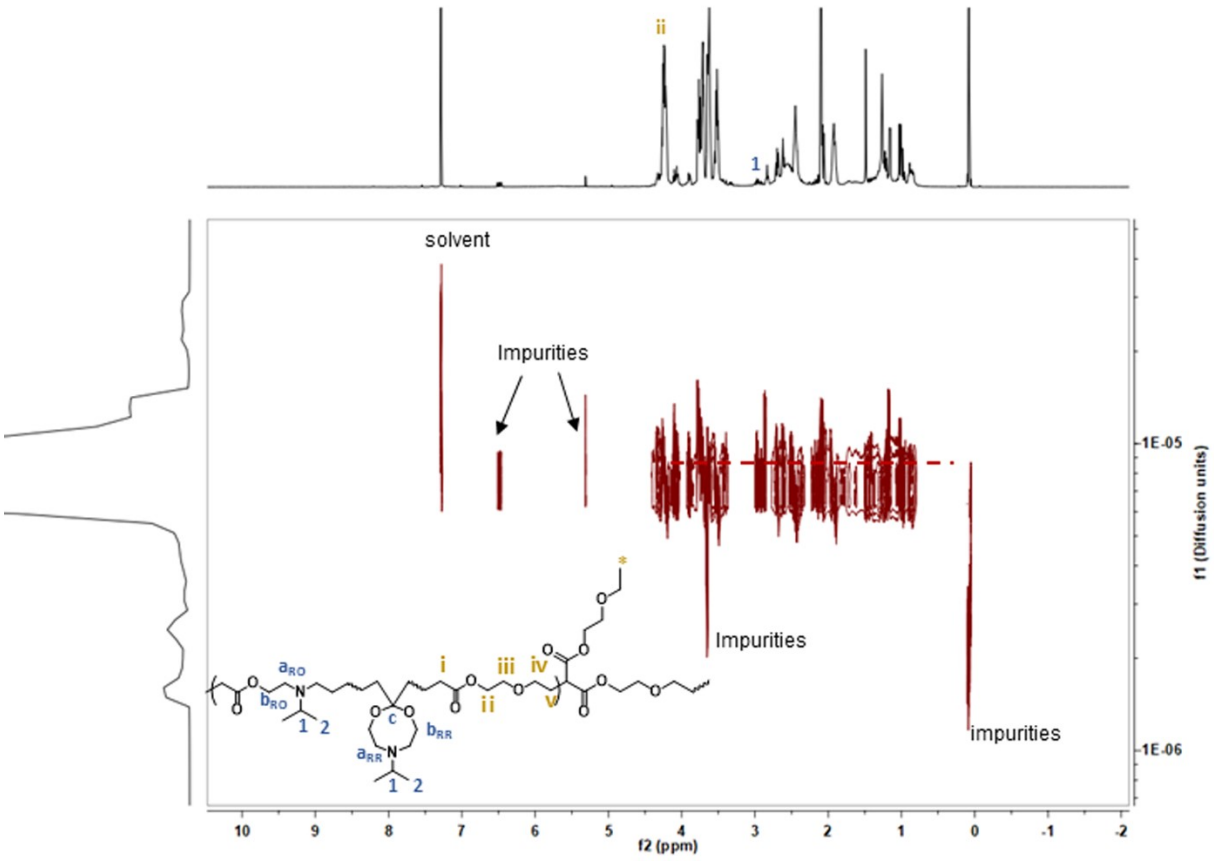

Figure S26. DOSY spectra of P(*i*Pr-MAC-co-MTC) with final molar fraction of *i*Pr-MAC/MTC: 10/90. The signal between 6.4-6.5 ppm could be attributed to the impurities during MTC preparation.

3.7 2D NMR measurements of P(*i*Pr-MAC-co-MTC)

^{1}H NMR and 2D NMR (COSY and HSQC) spectra of copolymer *i*Pr-MAC-5T were displayed as follows:

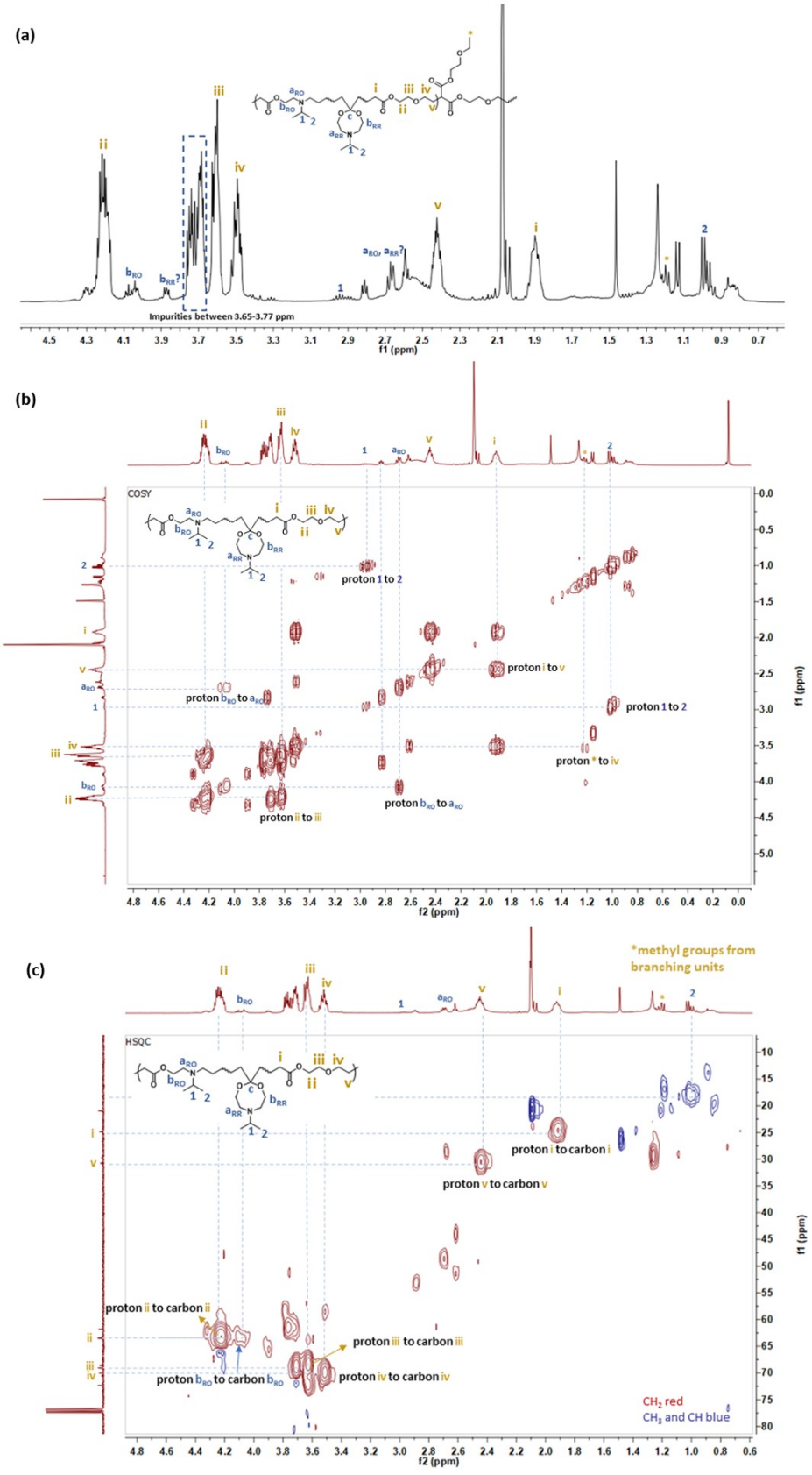

Figure S27. (a) ^{1}H NMR spectrum of copolymer *i*Pr-MAC-5T. 2D NMR spectra are shown in (b) from COSY experiments and in (c) from HSQC experiments of copolymer *i*Pr-MAC-5T.

To see the ^{i}Pr-MAC motifs clearly, 2D NMR spectra from HMBC experiments of ^{i}Pr-MAC-25T were conducted as supplement. In order to ensure good sample concentration for NMR measurements, two batches of copolymers ^{i}Pr-MAC-25T were mixed and subjected to HMBC measurements in combination. The signal assignment should be hence considered with caution owing to the unknown additional branching sites and combinations of ring-opened and ring-retaining structures.

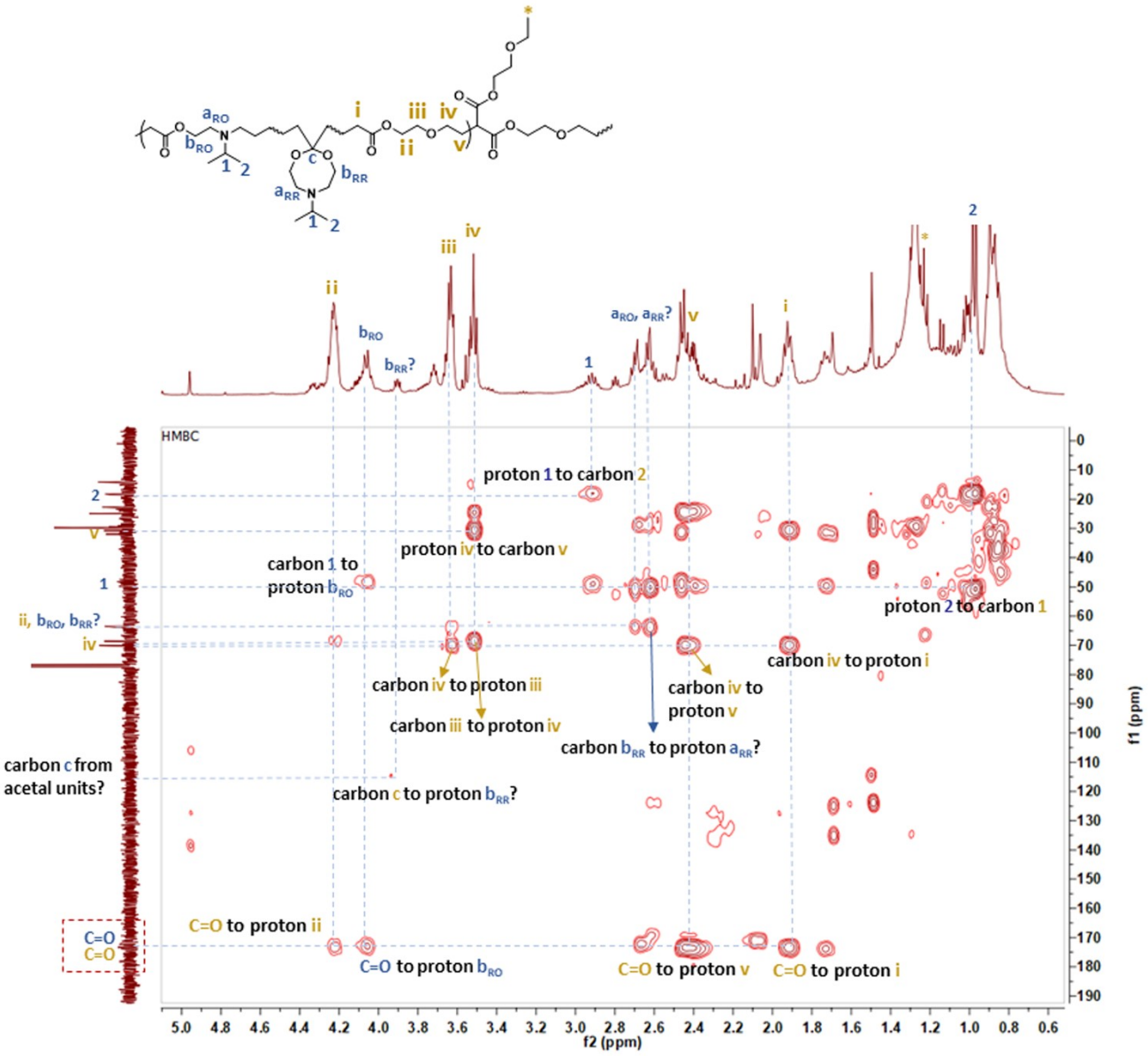

Figure S28. 2D NMR spectrum of an HMBC experiment of copolymer ^{i}Pr-MAC-25T.

3.8 SEC measurements of poly(*i*Pr-MAC-co-MTC)

All the samples were measured for two times and corresponding results were recorded in **Table S12**.

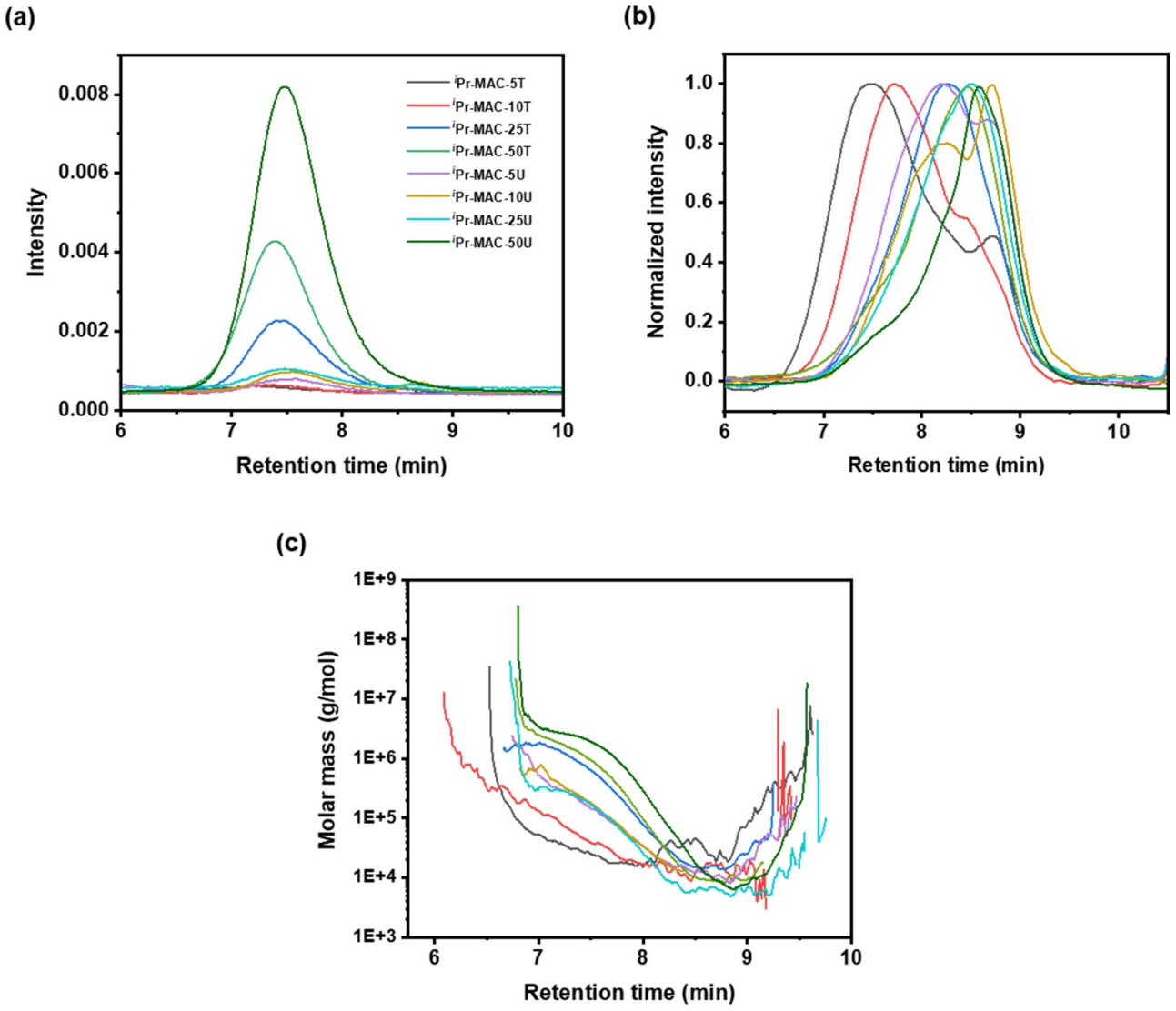

Figure S29. (a) Non-normalised light scattering, (b) normalised refractive index signals of poly(*i*Pr-MAC-co-MTC) and (c) evolution of molar mass with retention time detected by MALLS detector. All graphs have the same color code in the assignment to the copolymer and the caption is only shown in part (a).

3.9 Conversion of Alk-MAC and MTC

^{s}Bu-MAC-25T was selected as example:

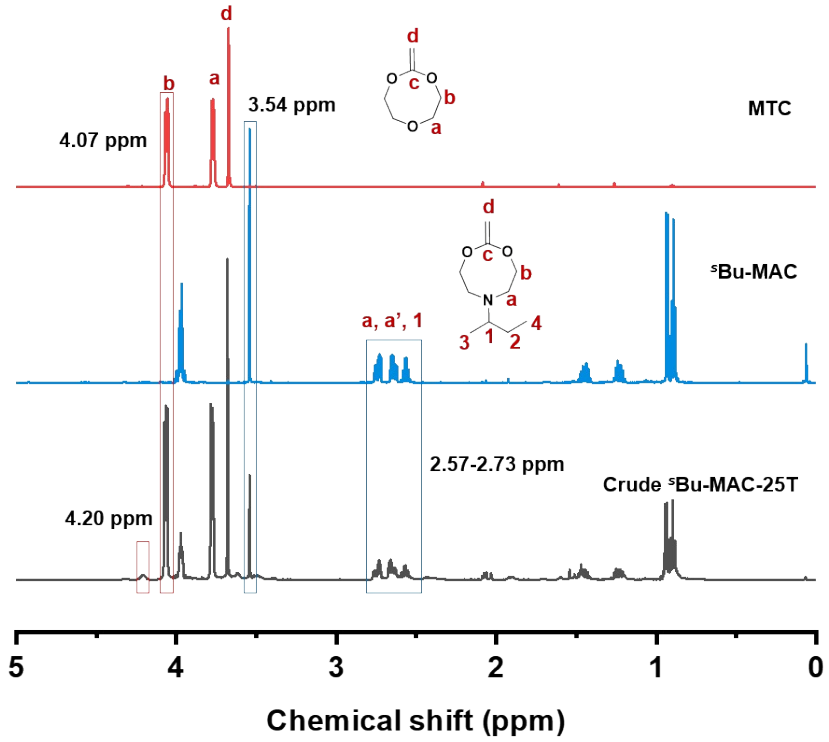

Figure S30. ^{1}H NMR spectra of MTC, ^{s}Bu-MAC **7e** and ^{s}Bu-MAC-25T crude product.

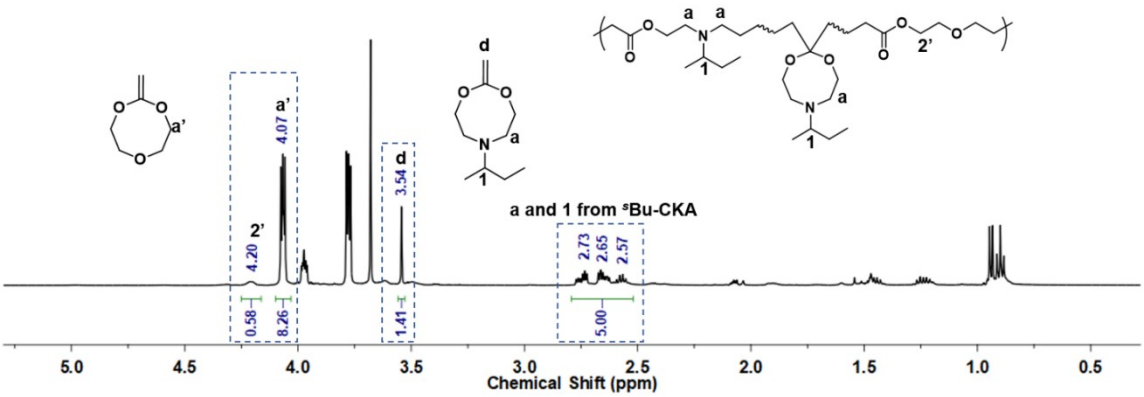

Figure S31. ^{1}H NMR spectrum of ^{s}Bu-MAC-25T crude product.

The conversion of MTC was calculated as aforementioned. When calculating conversion of ^{s}Bu-MAC **7e**, signals positioned from 2.57 to 2.73 ppm (representing protons **a** and **1**) were taken as reference (Figure S30). The conversion was calculated as follows:

$$\text{conversion } s\text{Bu - MAC} = \left(1 - \frac{5 \times \text{I}(3.54\ \text{ppm})}{2 \times \text{I}(2.57 - 2.73\ \text{ppm})}\right) \times 100\%$$

In Figure S31, conversion of MTC and ^{s}Bu-MAC were calculated for 12 and 29% respectively.

Conversion of MTC/Alk-MAC were calculated and summarized in **Table 1** in the main text.

3.10 ^{1}H NMR of purified poly(Alk-MAC-co-MTC)

Final molar fraction of MTC/Alk-MAC of each sample was calculated and summarized in Table 1 in the main text.

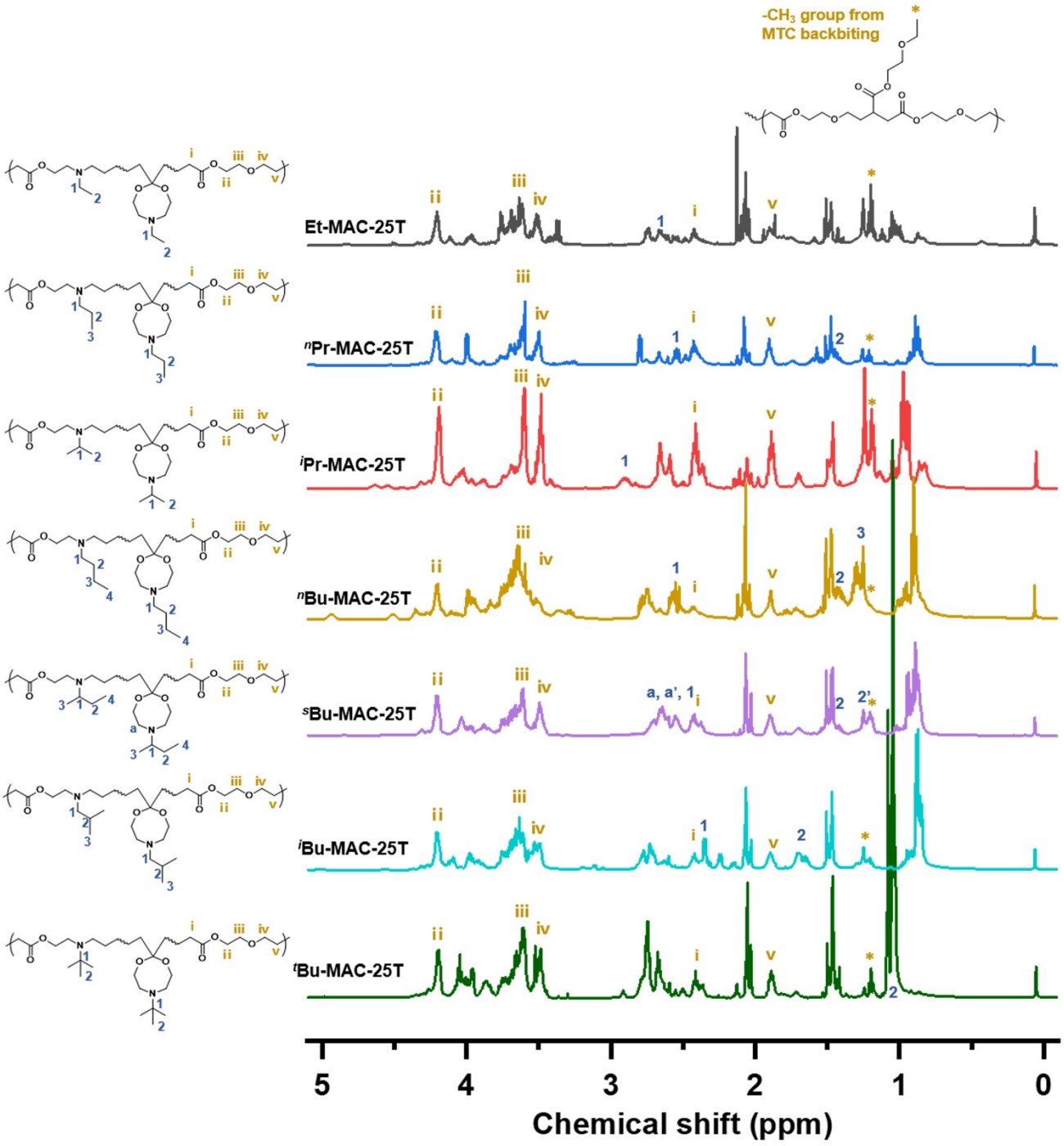

Figure S32. ^{1}H NMR spectra and possible signal assignment of poly(Alk-MAC-co-MTC) copolymers prepared through thermal polymerization (feed ratio of Alk-MAC/MTC = 25/75). * methyl group from the terminal of each MTC branching units, caused by MTC backbiting.[4]

3.11 ^{13}C NMR of poly(Alk-MAC-co-MTC)

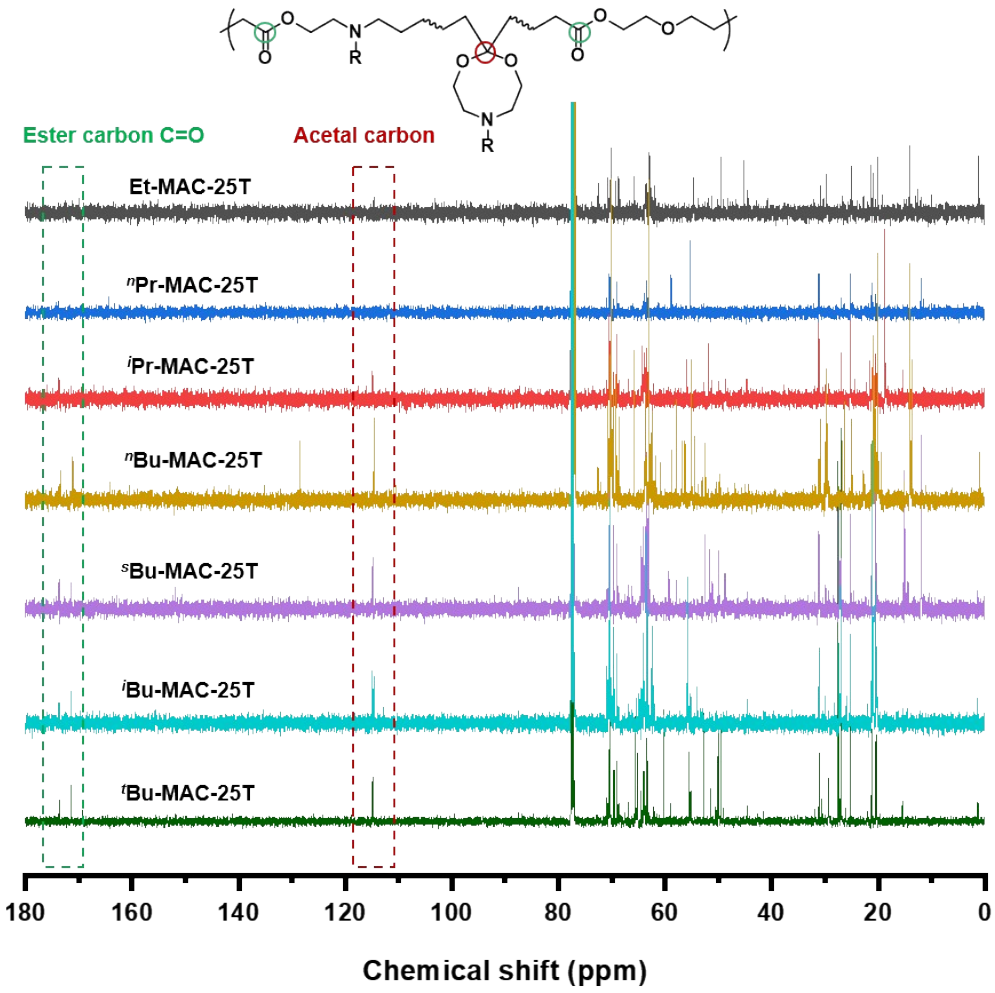

Figure S33. ^{13}C NMR spectra of poly(Alk-MAC-co-MTC) copolymers prepared through thermal polymerization (feed ratio Alk-MAC/MTC = 25/75). Signals at 171-173.6 ppm are attributed to the carbonyl of ester units of ring-opening structure and signals around 114.6 ppm are related to the acetal from ring-retaining units.[2]

3.12 ATR-FTIR spectrum of Et-MAC-25T

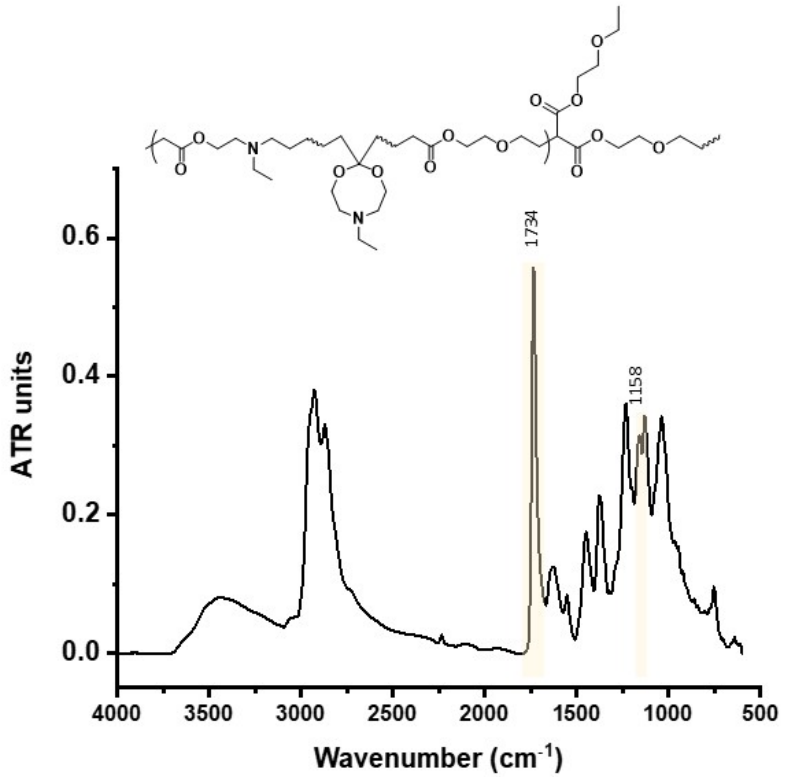

Figure S34. ATR-FTIR spectrum of copolymer Et-MAC-25T recorded at room temperature, with 4 cm^{-1} spectral resolution, showing C=O ester stretching at 1734 cm^{-1} and C-O stretching of ester units at 1158 cm^{-1}.

3.13 SEC measurements of poly(Alk-MAC-co-MTC)

All the samples were measured for two times and corresponding results were recorded in Table S12.

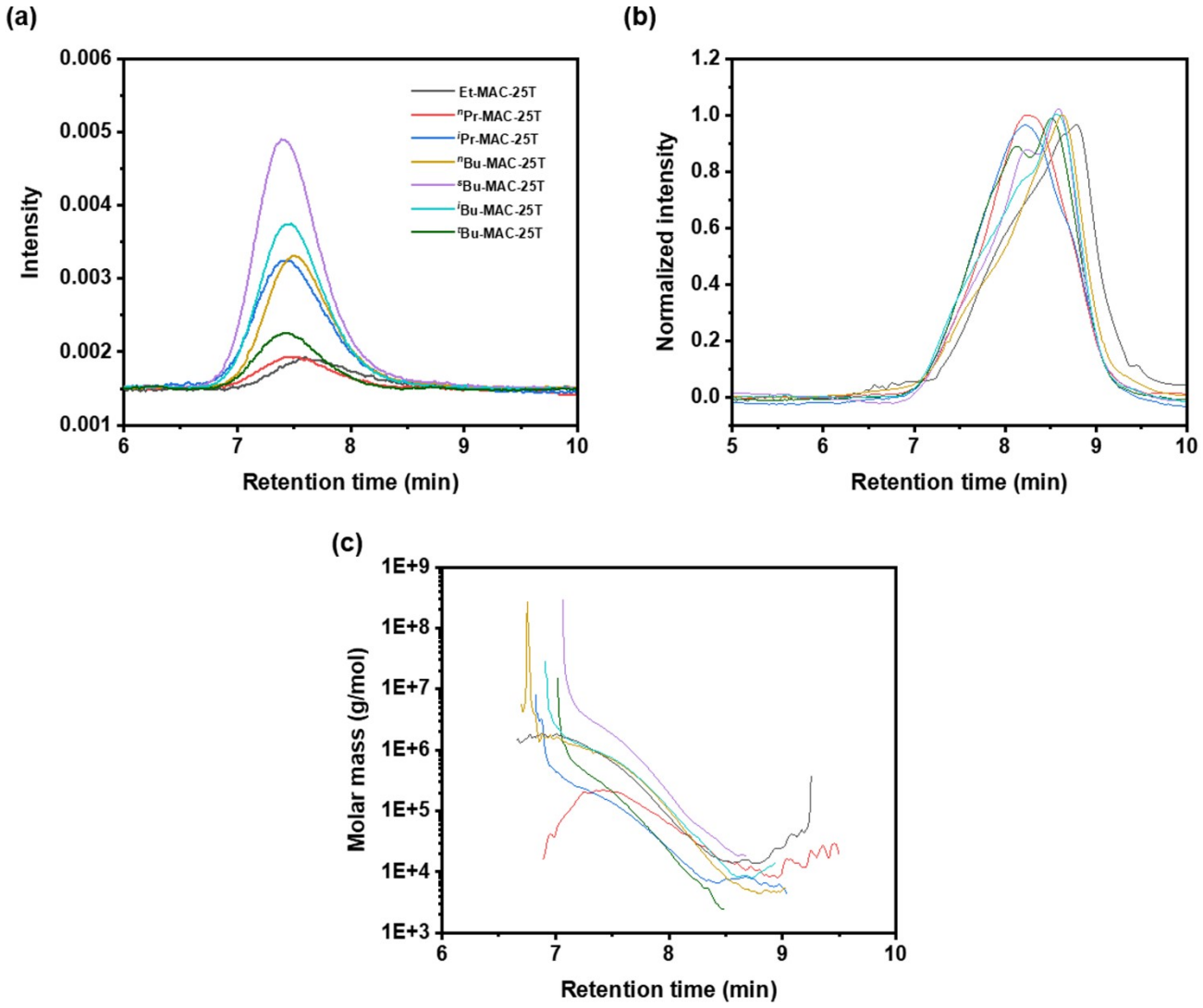

Figure S35. (a) Non-normalised light scattering, (b) normalised refractive index signals of poly(Alk-MAC-co-MTC) and (c) molar mass as a function of the retention time detected by MALLS detector. All graphs have the same color code in the assignment to the copolymer and the caption is only shown in part (a).

3.14 Molar mass and polymer dispersity of poly(Alk-MAC-co-MTC)

Table S12 listed M_n, M_w, dispersity and d*n*/d*c* values of all the copolymers. M_n, M_w and dispersity values were discussed in the main text

Table S12. Molar mass and polymer dispersity of poly(Alk-MAC-co-MTC)

Sample	M_n (kg/mol)	M_w (kg/mol)	Đ	d*n*/d*c*
^{i}Pr-MAC-5T	25.8	32.9	1.3	0.027
^{i}Pr-MAC-10T	26.6	43.5	1.6	0.027
^{i}Pr-MAC-25T	32.2	155	4.8	0.030
^{i}Pr-MAC-50T	18.2	193	11	0.042
^{i}Pr-MAC-5U	16.3	47.4	2.9	0.030
^{i}Pr-MAC-10U	29.3	68.2	2.3	0.038
^{i}Pr-MAC-25U	9.2	31.5	3.4	0.039
^{i}Pr-MAC-50U	16.5	248	15	0.048
Et-MAC-25T	17.8	44.8	2.5	0.032
^{n}Pr-MAC-25T	15.3	42.4	2.8	0.033
^{n}Bu-MAC-25T	11.8	126	11	0.035
^{s}Bu-MAC-25T	49.1	420	8.6	0.027
^{i}Bu-MAC-25T	21.5	183	8.5	0.032
^{t}Bu-MAC-25T	10.8	65.4	6.1	0.035

3.15 UV-vis transmittance measurements of copolymers

Two attempts were adopted to evaluate pK_a^*. Copolymer solutions of all substituents were measured as triplicates and first fitted into a Boltzmann equation individually in order to get average pK_a^* values and error margins (see in Figure S36-45 left side). In another case, all the plots measured were combined to undergo Boltzmann fitting (see in Figure S36-45 right side). The fitted Boltzmann equations were normalised and analysed in the main text (Figure 3). The corresponding pK_a^* values of respective copolymers obtained through both attempts can be seen in the Table S13.

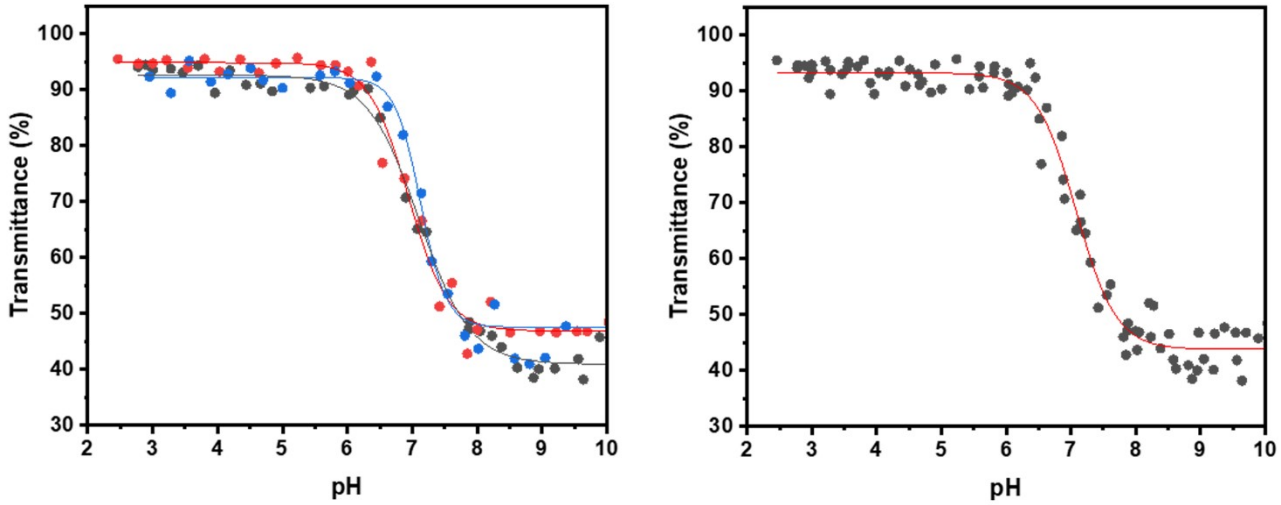

Figure S36. Left side: evolution of % transmittance of ^{i}Pr-MAC-25T solution with pH value variation. Right side: the fitted Boltzmann equation y = 43.76 + (93.25-43.76)/(1 + exp((x-7.08)/0.31))

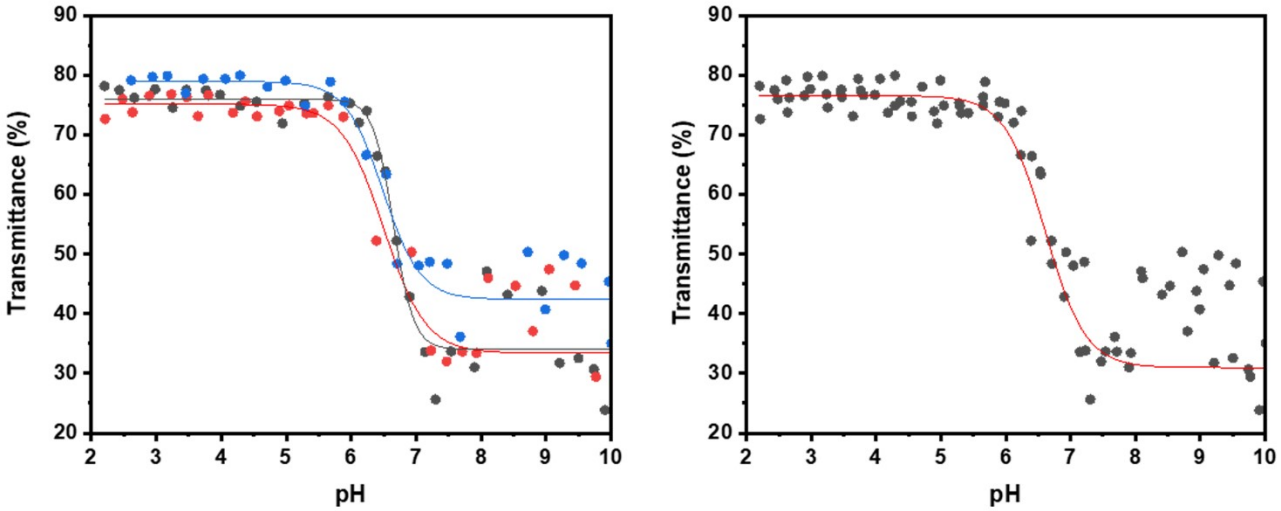

Figure S37. Left side: evolution of % transmittance of ^{i}Pr-MAC-50T solution with pH value variation. Right side: the fitted Boltzmann equation y = 30.96 + (76.56-30.96)/(1 + exp((x-6.61)/0.31))

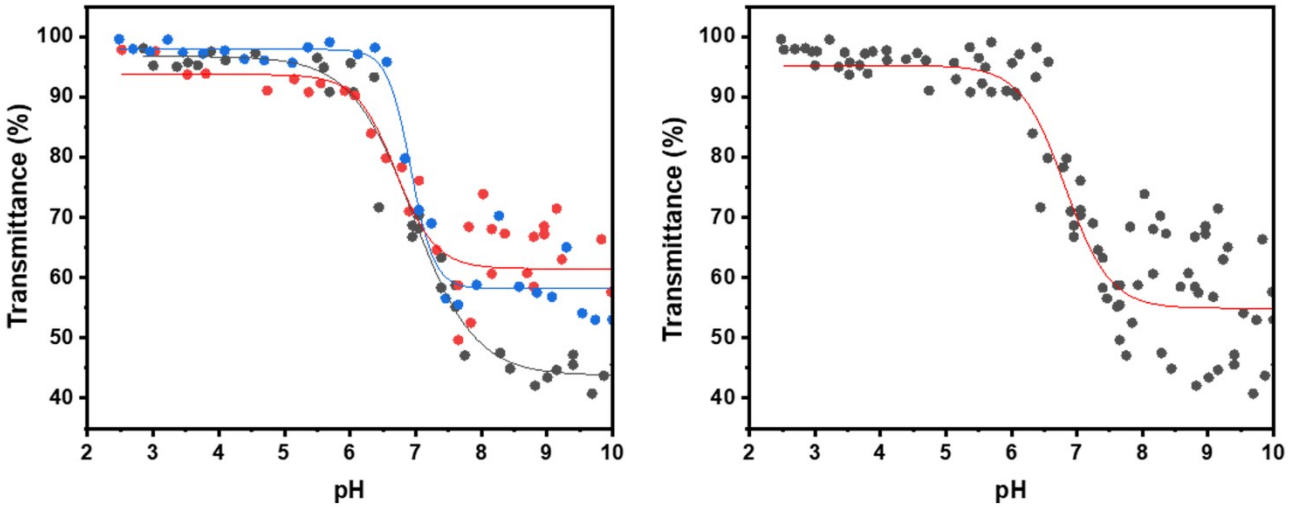

Figure S38. Left side: evolution of % transmittance of ^{i}Pr-MAC-25U solution with pH value variation. Right side: the fitted Boltzmann equation y = 54.90 + (95.22-54.90)/(1 + exp((x-6.82)/0.34))

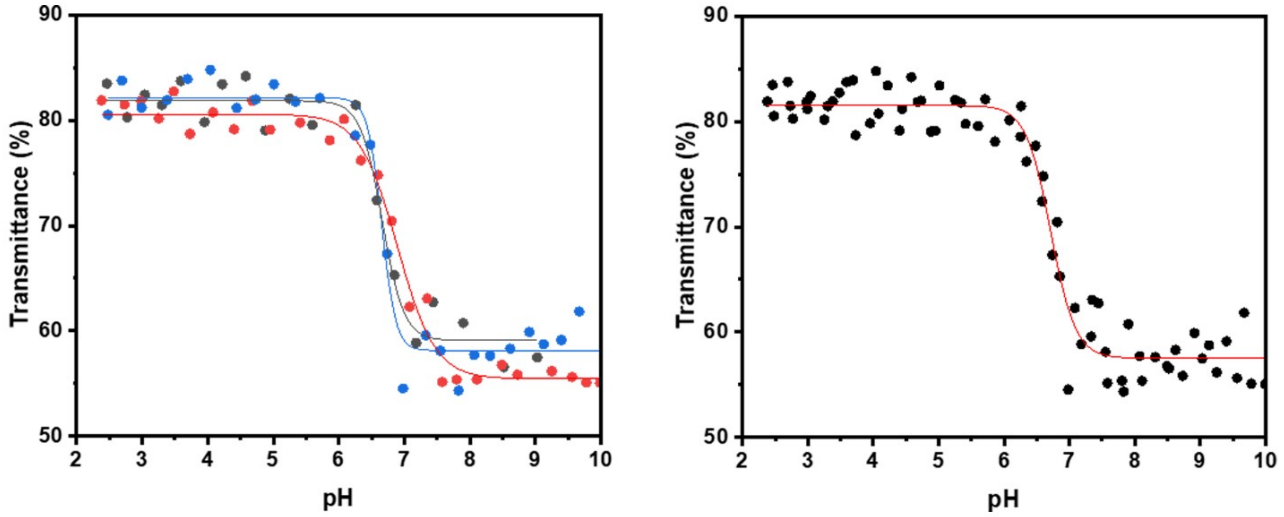

Figure S39. Left side: evolution of % transmittance of ^{i}Pr-MAC-50U solution with pH value variation. Right side: the fitted Boltzmann equation y = 57.52 + (81.52-57.52)/(1 + exp((x-6.71)/0.19)

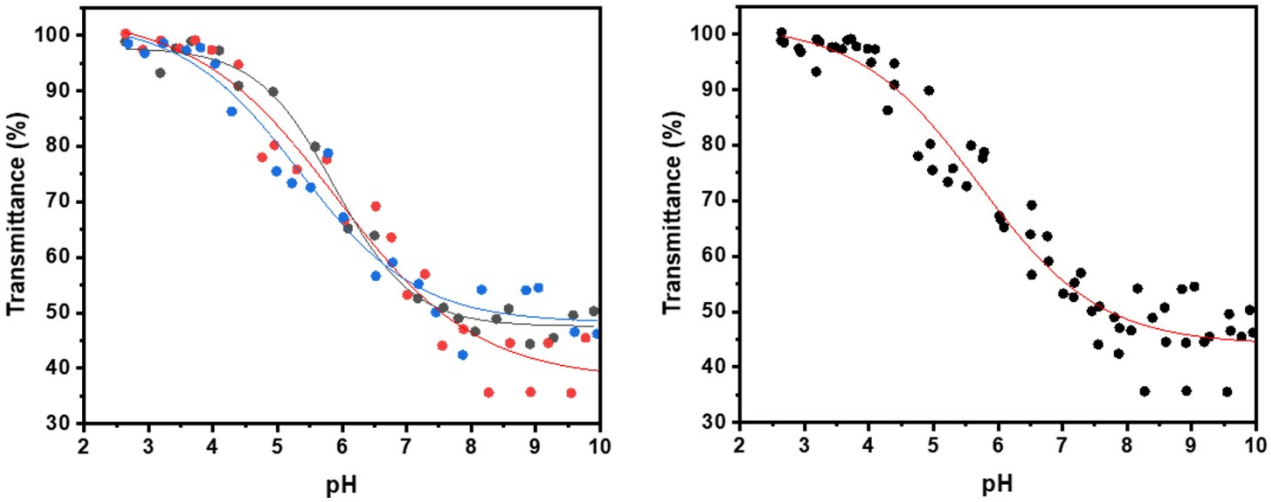

Figure S40. Left side: evolution of % transmittance of Et-MAC-25T solution with pH value variation. Right side: the fitted Boltzmann equation y = 44.07 + (101.79-44.07)/(1 + exp((x-5.70)/0.94))

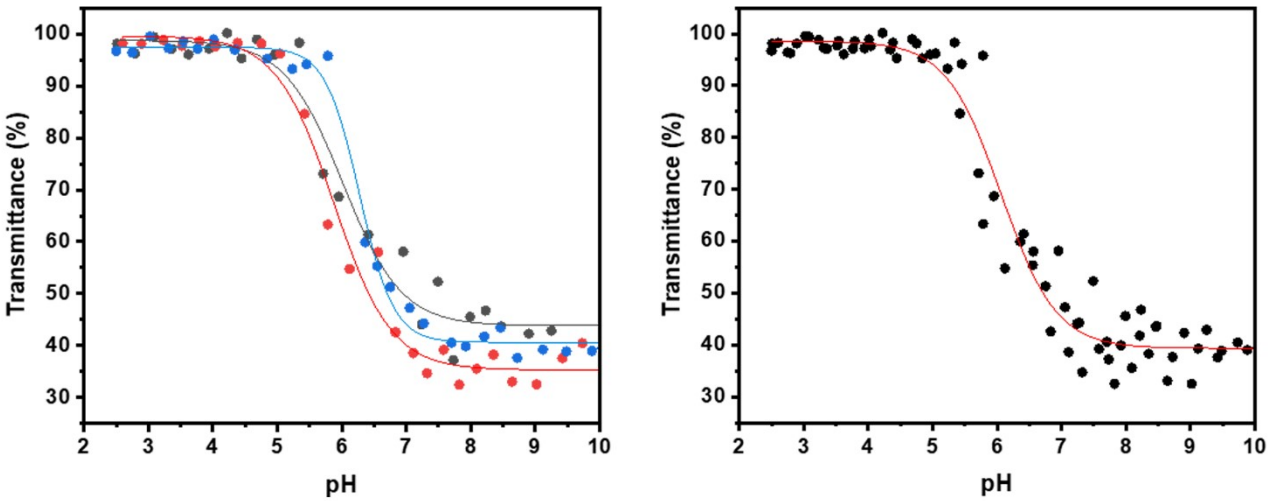

Figure S41. Left side: evolution of % transmittance of ^{n}Pr-MAC-25T solution with pH value variation. Right side: the fitted Boltzmann equation y = 39.33 + (98.58-39.33)/(1 + exp((x-6.06)/0.43))

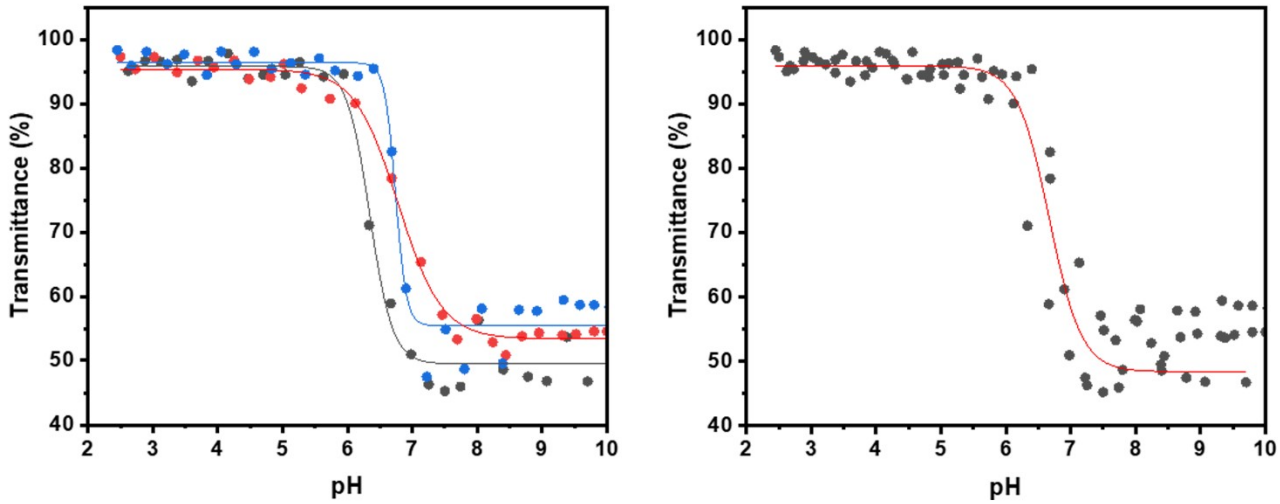

Figure S42. Left side: evolution of % transmittance of ^{n}Bu-MAC-25T solution with pH value variation. Right side: the fitted Boltzmann equation y = 48.40 + (95.89-48.40)/(1 + exp((x-6.67)/0.25))

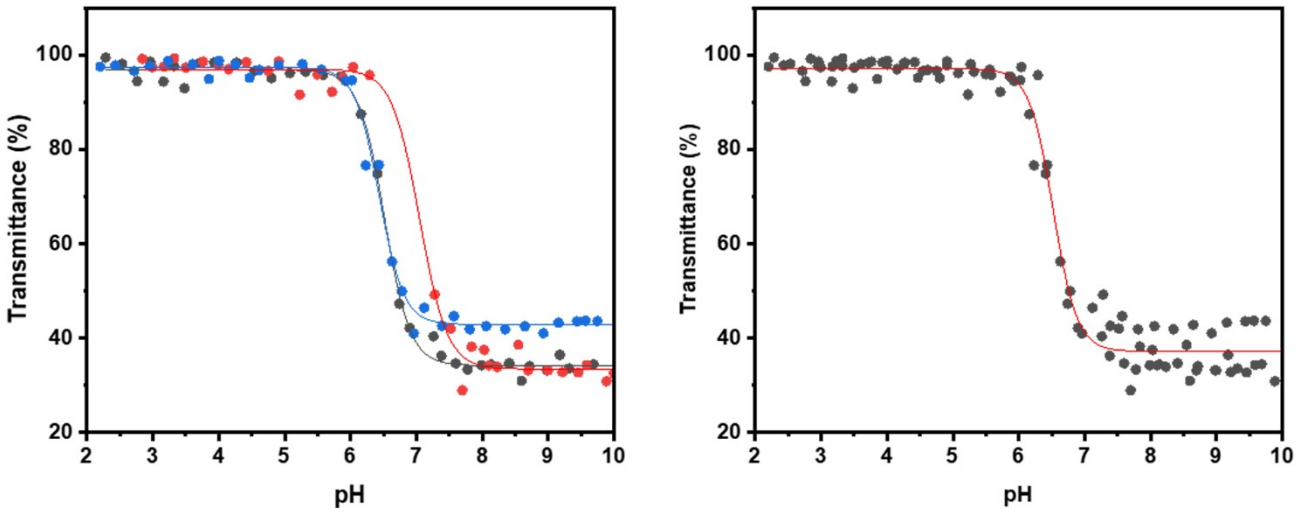

Figure S43. Left side: evolution of % transmittance of ^{s}Bu-MAC-25T solution with pH value variation. Right side: the fitted Boltzmann equation y = 37.21 + (97.11-37.21)/(1 + exp((x-6.52)/0.183))

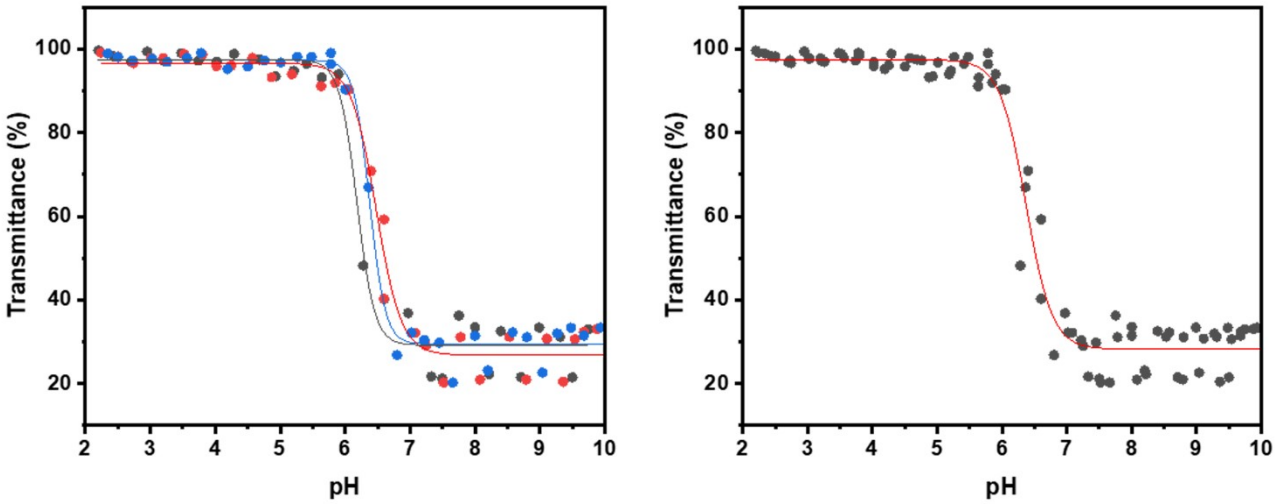

Figure S44. Left side: evolution of % transmittance of ^{i}Bu-MAC-25T solution with pH value variation. Right side: the fitted Boltzmann equation y = 28.22 + (97.42-28.22)/(1 + exp((x-6.37)/0.20))

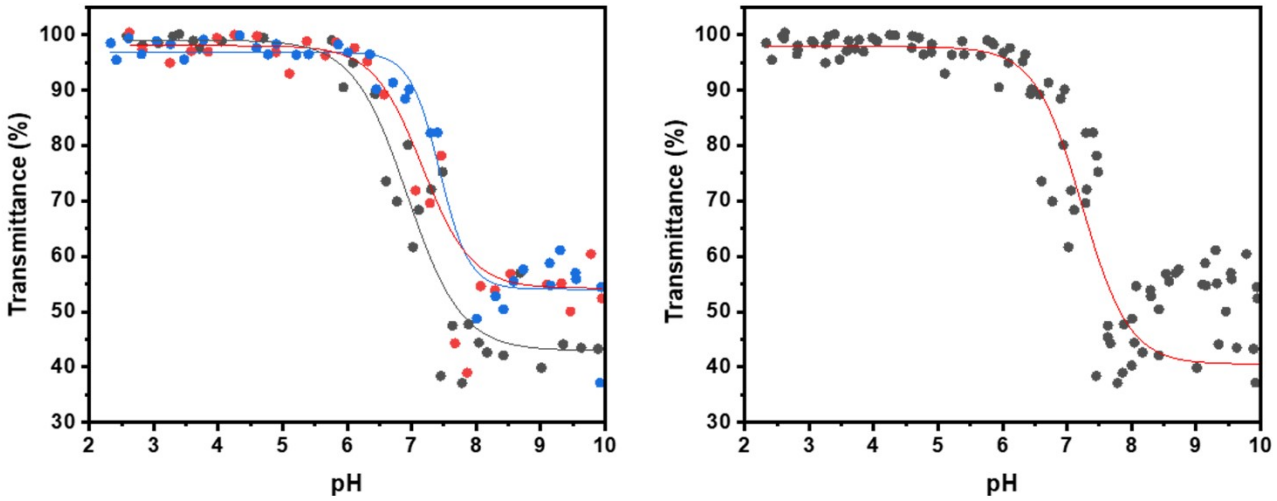

Figure S45. Left side: evolution of % transmittance of ^{t}Bu-MAC-25T solution with pH value variation. Right side: the fitted Boltzmann equation y = 40.52 + (97.83-40.52)/(1 + exp((x-7.23)/0.37))

Table S13. pK_a^* values of poly(Alk-MAC-co-MTC) measured by two attempts

Sample	pK_a^*1	pK_a^*2	pK_a^*3	$pK_a^*_{average}$	$pK_a^*_{combined}$
^{i}Pr-MAC-25T	7.1	6.9	7.1	7.0±0.1	7.1
^{i}Pr-MAC-50T	6.5	6.6	6.5	6.5±0.1	6.6
^{i}Pr-MAC-25U	7.0	6.7	6.9	6.9±0.2	6.9
^{i}Pr-MAC-50U	6.6	6.9	6.7	6.7±0.2	6.7
Et-MAC-25T	5.9	5.4	5.9	5.7±0.3	5.7
^{n}Pr-MAC-25T	6.0	5.9	6.3	6.1±0.2	6.1
^{n}Bu-MAC-25T	6.3	6.8	6.7	6.6±0.3	6.7
^{s}Bu-MAC-25T	6.5	6.4	7.0	6.6±0.3	6.5
^{i}Bu-MAC-25T	6.5	6.4	6.2	6.4±0.2	6.4
^{t}Bu-MAC-25T	6.9	7.2	7.4	7.2±0.3	7.2

3.16 DLS measurement of ^{i}Pr-MAC-25T solution

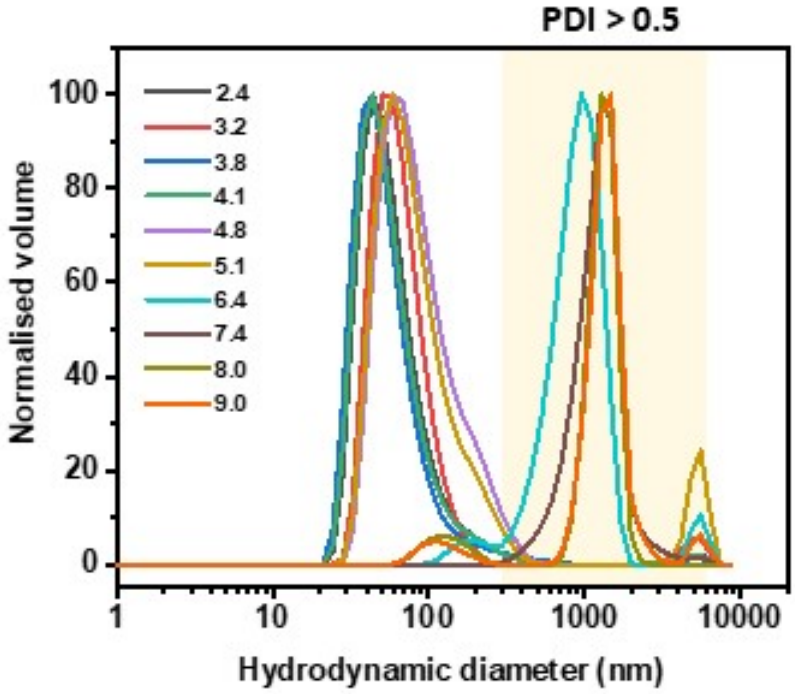

Figure S46. DLS measurements of ^{i}Pr-MAC-25T solution during deprotonation process. Volume size distribution curves showed a significant increase in size with the increase of pH value from 2.4 to 9.

3.17 Hydrolytic degradation of copolymers

The hydrolytic degradation process was introduced in the measurements section. After degradation, the mixture was characterized through NMR spectroscopy.

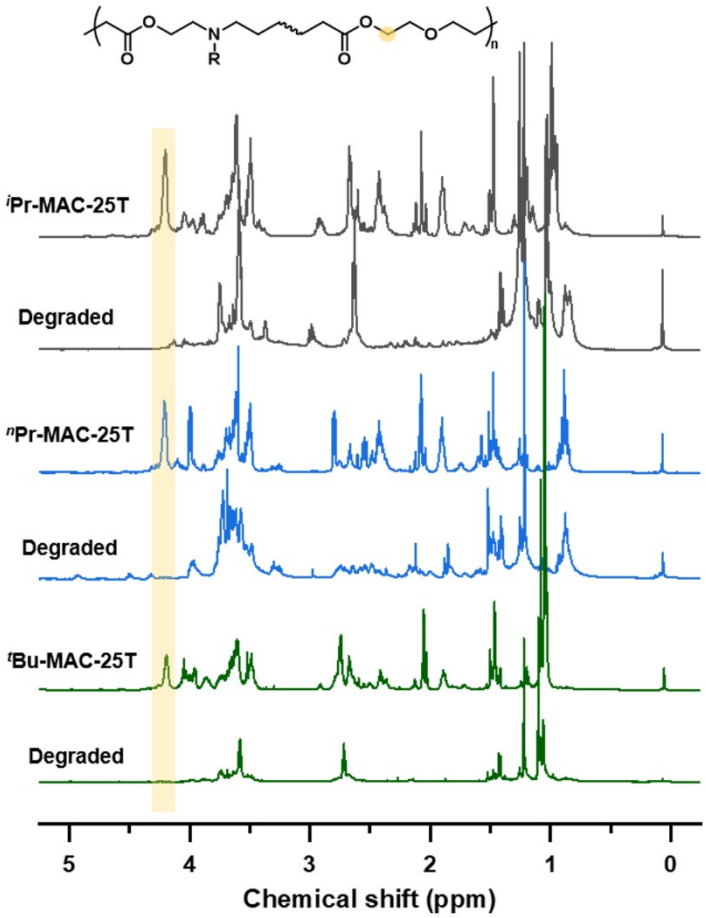

Figure S47. ^{1}H NMR spectra of ^{i}Pr-MAC-25T, ^{n}Pr-MAC-25T and ^{t}Bu-MAC-25T before and after hydrolytic degradation.

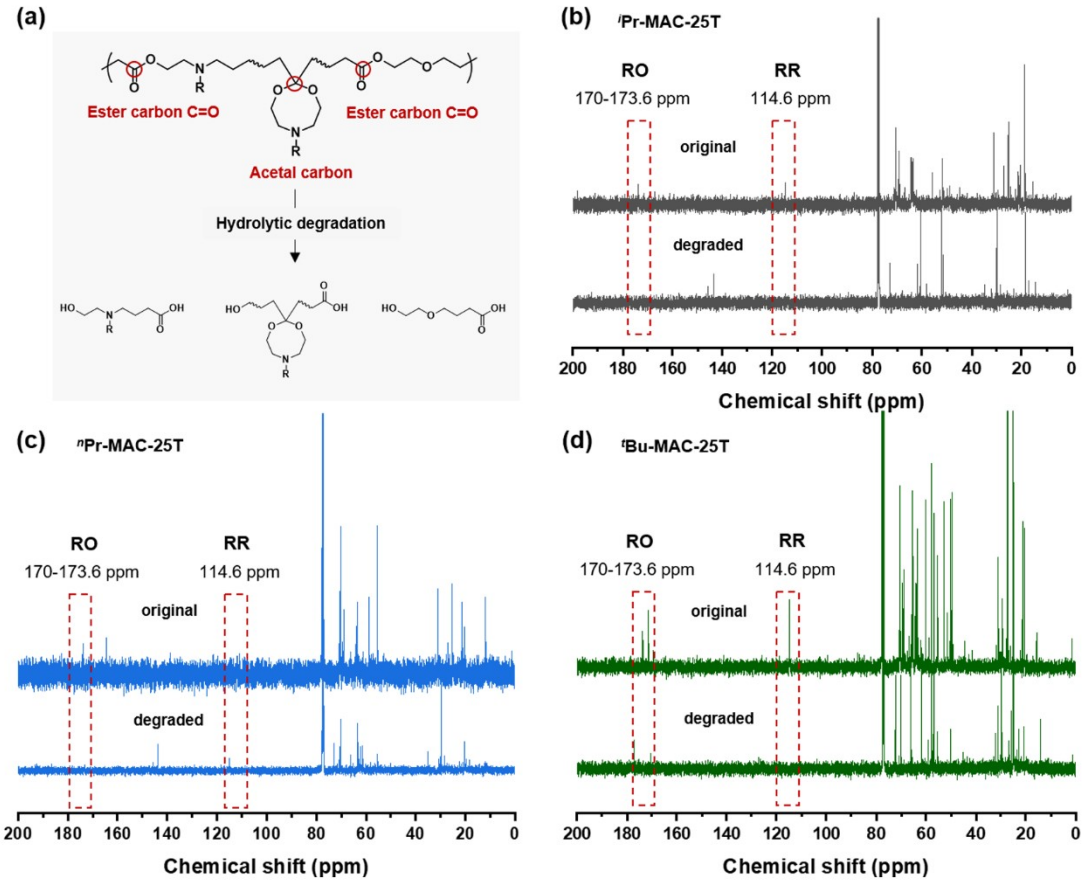

Figure S48. (a) Possible chemical structure of poly(Alk-MAC-co-MTC) copolymers and the possible substances after subjected to hydrolytic degradation. ^{13}C NMR spectra of (b) ^{i}Pr-MAC-25T, (c) ^{n}Pr-MAC-25T and (d) ^{t}Bu-MAC-25T before and after hydrolytic degradation.

To extract the small molecules after degradation, the organic solvent was removed under reduced pressure and then the degraded copolymer was dissolved into D_2O for ^1H NMR characterization. ^{i}Pr-MAC-25T was selected as example (Figure S49) and the ester-protons **ii** at 4.17-4.20 ppm disappeared completely, again confirmed the degradation of copolymer.

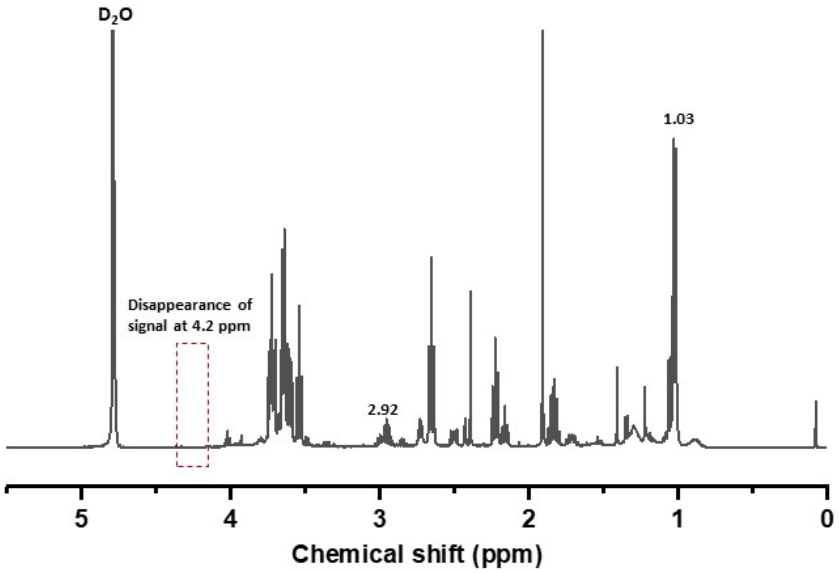

Figure S49. ^1H NMR spectrum of degraded ^{i}Pr-MAC-25T measured in D_2O.

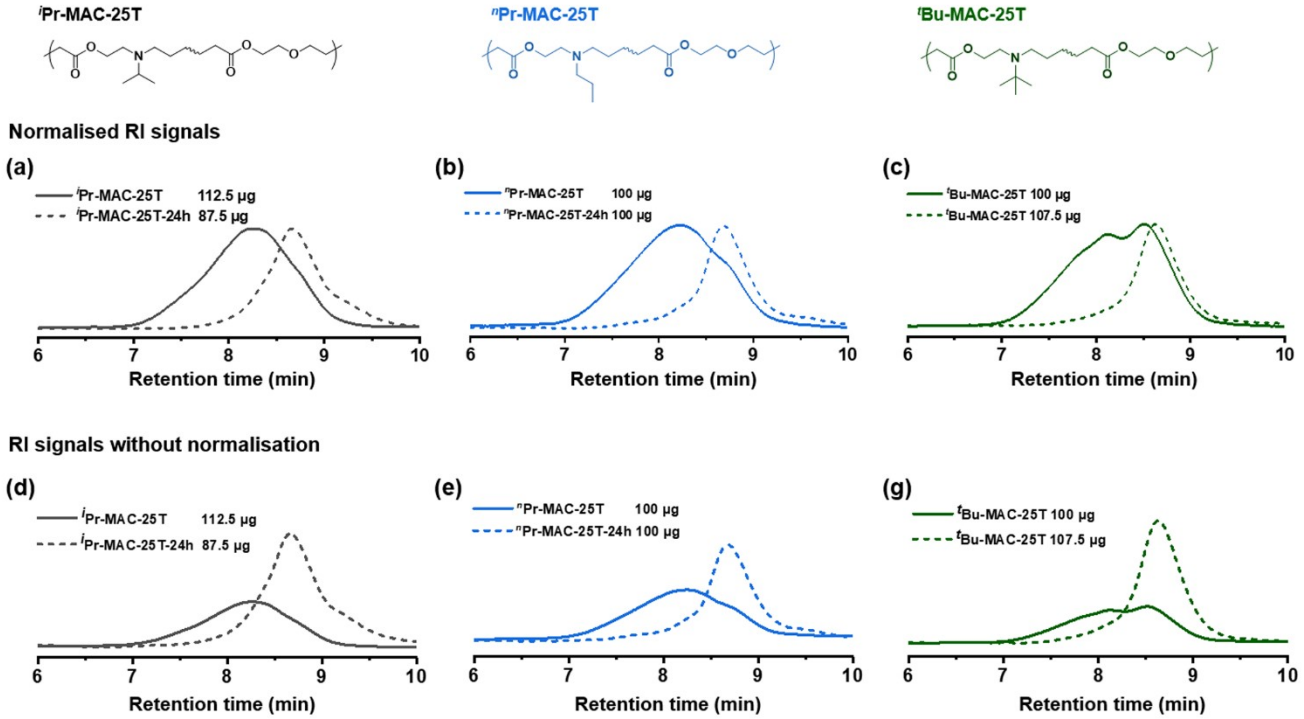

Figure S50. Normalised refractive index chromatograms of original and degraded copolymers (a) ^{i}Pr-MAC-25T, (b) ^{n}Pr-MAC-25T and (c) ^{t}Bu-MAC-25T. The non-normalised refractive index chromatograms of original and degraded copolymers (d) ^{i}Pr-MAC-25T, (e) ^{n}Pr-MAC-25T and (g) ^{t}Bu-MAC-25T. The mass represented the inject molar mass of corresponding sample during SEC measurements.

4 References

1. M. W. Schmidt, K. K. Baldridge, J. A. Boatz, S. T. Elbert, M. S. Gordon, J. H. Jensen, S. Koseki, N. Matsunaga, K. A. Nguyen, S. Su, T. L. Windus, M. Dupuis and J. A. Montgomery Jr, *J. Comput. Chem.*, 1993, **14**, 1347-1363.
2. J. Folini, C.-H. Huang, J. C. Anderson, W. P. Meier and J. Gaitzsch, *Polym. Chem.*, 2019, **10**, 5285-5288.
3. J. Undin, P. Plikk, A. Finne-Wistrand and A.-C. Albertsson, *J. Polym. Sci., Part A: Polym. Chem.*, 2010, **48**, 4965-4973.
4. T. Pesenti, E. Gillon, S. Ishii, S. Messaoudi, Y. Guillaneuf, A. Imberty and J. Nicolas, *Biomacromolecules*, 2023, **24**, 991-1002.